

~~SECURITY INFORMATION~~ SECURITY INFORMATION

222
Copy
RM L53A13

NACA RM L53A13



RESEARCH MEMORANDUM

L402

INVESTIGATIONS OF THE DAMPING IN ROLL OF SWEPT AND
TAPERED WINGS AT SUPERSONIC SPEEDS

By Russell W. McDearmon and Harry S. Heinke, Jr.

Langley Aeronautical Laboratory
Langley Field, Va.

CLASSIFIED DOCUMENT

NATIONAL ADVISORY COMMITTEE
FOR AERONAUTICS

WASHINGTON

March 3, 1953

RECEIPT SIGNATURE
REQUIRED

319.98/13

1T

NACA RM 153A13



0144397



NATIONAL ADVISORY COMMITTEE FOR AERONAUTICS

RESEARCH MEMORANDUM

INVESTIGATIONS OF THE DAMPING IN ROLL OF SWEPT AND
TAPERED WINGS AT SUPERSONIC SPEEDS

By Russell W. McDearmon and Harry S. Heinke, Jr.

SUMMARY

Experimental damping-in-roll derivatives have been obtained for a series of 33 swept and tapered wings. The wing plan forms were selected so that a range of leading-edge positions ahead of and behind the Mach cone was obtained at three Mach numbers, 1.62, 1.93, and 2.41.

The damping in roll appeared to be predicted quite accurately by the linear theory when the wing leading edges were well ahead of the Mach cones emanating from the wing apexes. When the leading edges were in the vicinity of or behind the Mach cones, the experimental damping in roll was considerably less than that predicted by theory. Poorer agreement with theory was obtained for the wings having a taper ratio of 0.25 with leading edges behind or in the vicinity of the Mach cone than for the wings having a taper ratio of 0 with the same leading-edge positions relative to the Mach cone.

A minor investigation was made of the effects of thickness on the damping in roll. It was found that the damping in roll of the thin wings agreed more closely with theory than that of the thicker wings of identical plan forms. The difference in the damping in roll for the wings of different thicknesses but identical plan forms was greater when the leading edges were behind the Mach cone than when the leading edges were ahead of the Mach cone.

INTRODUCTION

An important factor in stability and control calculations for aircraft and missiles is the aerodynamic resistance to roll, or damping in roll. The damping in roll is generally expressed in terms of the non-dimensional parameter C_{l_p} , which is the rate of change of rolling-moment coefficient, C_l , with change of wing-tip helix angle, $\theta_b/2V$.

The linear theory of supersonic flow has provided damping-in-roll predictions for a large class of wing plan forms (see refs. 1 to 5). However, the experimental information presently available on the rolling characteristics of wings at supersonic speeds is rather limited. The damping in roll of a group of rectangular and triangular wings at supersonic speeds was investigated in the Langley 9-inch supersonic tunnel (ref. 6). Free-flight investigations utilizing rocket-propelled test vehicles have been made of the damping in roll of several wings, including a triangular-wing configuration geometrically similar to one of those used in reference 6 (see ref. 7). Numerous other free-flight tests utilizing rocket-propelled vehicles have been made of the rolling characteristics of various wing-body and wing-body-tail combinations, including those reported in references 8, 9, and 10.

The purpose of the present investigation was to supply experimental values of C_{l_p} for a series of 33 swept and tapered wings and to compare them with theoretical predictions. For 31 of the wings the leading- and trailing-edge sweep angles and taper ratios were varied systematically, and the thickness was held constant. Also two thinner wings were constructed to study thickness effects on C_{l_p} . The plan forms selected gave data through the leading-edge-sweep-angle range such that the leading edge passed from behind to ahead of the Mach cone emanating from the wing apices. The taper ratios were 0 and 0.25.

All wings were mounted on a small cylindrical sting and were tested at Mach numbers of 1.62, 1.93, and 2.41. The Reynolds number range of the tests was from 0.52×10^6 to 2.37×10^6 , based on the wing mean aerodynamic chord.

SYMBOLS

b	wing span
S	total wing area
A	aspect ratio, b^2/S
c_r	wing root chord (calculated from measured wing dimensions)
c_t	wing tip chord
λ	wing taper ratio, c_t/c_r
Λ	angle of sweep of wing leading edge, positive for sweepback

Λ_{TE}	angle of sweep of wing trailing edge, positive for sweepback
M	free-stream Mach number
$\beta = \sqrt{M^2 - 1}$	
μ	Mach angle, $\sin^{-1} \frac{1}{M}$
ρ	angular rolling velocity
q	free-stream dynamic pressure
R	Reynolds number based on mean aerodynamic chord of wing
t	maximum wing thickness
V	free-stream velocity
$p_b/2V$	helix angle generated by wing tip in roll
L	rolling moment
C_l	rolling-moment coefficient, L/qSb
C_{l_p}	damping-in-roll derivative, $\partial C_l / \partial \frac{p_b}{2V}$

APPARATUS

Wind Tunnel

All tests were conducted in the Langley 9-inch supersonic tunnel, which is a continuous-operation closed-circuit type in which the stream pressure, temperature, and humidity conditions can be controlled and regulated. Different test Mach numbers are provided by interchangeable nozzle blocks which form test sections approximately 9 inches square. Throughout the present tests, the moisture content in the tunnel was kept sufficiently low so that the effects of condensation in the supersonic nozzle were negligible.

Models, Support, and Rolling-Moment Balance

The pertinent wing characteristics are presented in table I. All but two of the wings were constructed of 3/16-inch-thick, SAE 4130 steel

sheet. The remaining two (wings 10-A and 27-A), used to study thickness effects on C_{l_p} , were 1/8 inch thick and of the same material. The edges of the entire group were beveled at an angle of 5° in a direction parallel to the wing root chord. All surfaces were ground and polished to insure a smooth finish.

The wings were mounted on a small cylindrical sting by means of a tang inserted in a groove in the sting, and were secured by lock screws and pins. The gap at the wing-sting juncture was filled in with plaster.

Photographs of the damping-in-roll test apparatus are presented in figure 1. The sting on which the wings were mounted was connected to a shaft rotated by an air-driven impeller. Strain gages were so located on the shaft as to be sensitive only to a rolling moment applied by a wing. In operation this rolling moment was measured on a strain indicator unit which was wired to the rolling-moment strain gages by means of slip rings and brushes. With minor exceptions, this unit was the same as the standard Baldwin Southwark SR-4 strain indicator unit.

The rolling velocity was measured with a Stroboconn frequency indicator which was modified to indicate revolutions per minute by means of a generator attached to the rear of the shaft.

TEST PROCEDURE

The models were rolled by means of a jet of compressed air directed against the impeller blades. The desired values of rolling velocity were obtained by varying the mass flow of the compressed air through a manual gate valve. The corresponding rolling moments were indicated on the strain-gage indicating unit.

The rolling-moment installation was calibrated statically before and at intervals during the testing to determine any possible changes in the strain-gage constant.

During a test of a given wing, the amount of air exhausting from the impeller into the tunnel exceeded the amount of air leaving through the bleed valve which vented the tunnel stagnation chamber to the atmosphere. The result was a temporary increase in the tunnel stagnation pressure (and dynamic pressure and Reynolds number). This occurred most noticeably for wings with large damping, since a greater mass flow of air through the impeller was required. In all cases the pressure was allowed to settle out to a constant value before data were taken.

PRECISION

The precision of the data has been determined by estimating the accuracies of the measured quantities and evaluating their effects on the coefficient C_l and the parameter $pb/2V$. Over the range of moments encountered in the tests, the maximum error in the strain-gage-balance calibration factor was ± 1.1 percent. The resulting error in C_l was ± 1.1 percent. Error in the measurement of the pertinent wing angles gave an uncertainty in wing area such that an error of about ± 0.5 percent was present in the values of C_l . Measurements of the rolling velocity were in error by ± 5 rpm in the test range and contributed a maximum error in $pb/2V$ of ± 0.4 percent. The surveyed variation of each of the free-stream Mach numbers is about ± 0.01 .

RESULTS AND DISCUSSION

The variations of rolling-moment coefficient with wing-tip helix angle for the 33 wings tested are presented in figures 2 to 6. Within the accuracy of the data, the values of C_l for most of the wings at the three Mach numbers varied linearly with the rolling velocity. The parameter C_{l_p} was therefore independent of rolling velocity, as predicted by linear theory.

For several of the slender wings having highly sweptback leading and trailing edges, the variations of C_l with $pb/2V$ were nonlinear (e.g., figs. 2(b), 3(a), 3(e), 3(f), 3(g), and 3(i)). These nonlinearities probably represent the net contributions to C_l of thickness effects, separation of the flow near the tips, and aeroelastic effects. Since the variations of C_l with $pb/2V$ were nonlinear for some of the wings, all slopes were estimated for that portion of the curve through a value of $pb/2V$ of 0.02.

The collected values of C_{l_p} are plotted in figures 7 to 12 in a manner suggested by the linear theory for wings in steady roll. The abscissa is the quantity $\beta \cot \Lambda$, which describes the position of the leading edges relative to the Mach cone from the wing apex. For values of $\beta \cot \Lambda$ greater than 1, the leading edge lies ahead of the Mach cone (supersonic leading edge); for values less than 1, the leading edge lies behind the Mach cone (subsonic leading edge). Plotted as the ordinate is the quantity βC_{l_p} . For all except the triangular wings the values of βC_{l_p} for wings having the same taper ratio and tested at Mach numbers giving a common value of βA are presented on the same

plot. For the triangular wings the values of βC_{l_p} at all three Mach numbers are presented on one plot. The figure plotted in this manner allows the theoretical values for isolated wings to be represented by a single curve independent of Mach number. The theoretical predictions of βC_{l_p} were obtained from references 1, 2, and 4, according to the geometric properties of the various wings.

For wings 1 to 28 (figs. 7 to 11), the damping in roll agreed quite closely with theoretical predictions for $\beta \cot \Lambda \geq 1.5$. For $\beta \cot \Lambda < 1.5$, the agreement of the damping in roll with theory became progressively less as $\beta \cot \Lambda$ decreased. For each value of βA , the poorest agreement with theory was found at the lowest value of $\beta \cot \Lambda$ obtained. The agreement was poorer for the wings having a taper ratio of 0.25 than for the wings having a taper ratio of 0; evidence of this is contained in the following table:

Approximate value of βA	Minimum value of $\beta \cot \Lambda$	Wing	Taper ratio	Mach no.	Experimental βC_{l_p}	
					Theoretical βC_{l_p}	Experimental βC_{l_p}
2.35	0.46	1 6	0 .25	1.62	0.804	
				1.62	.563	
3.00	.47	2 10	0 .25	1.62	.642	
				1.62	.382	
4.00	.61	2 10	0 .25	1.93	.555	
				1.93	.439	
5.00	.80	2 10	0 .25	2.41	.519	
				2.41	.403	
6.80	1.02	4 13	0 .25	2.41	.585	
				2.41	.482	

By referring to table I, it may be observed that the two wings compared at each value of βA had the same leading-edge-sweep angles and the same aspect ratios. Thus, the principal difference in the two was the difference in the areas of the tip regions. The poorer agreement with theory for the wings having a taper ratio of 0.25 was probably due to separation of the flow at the tips and thickness effects. Separation would cause a smaller pressure differential between the upper and lower surfaces than that predicted by theory; this, acting on a larger tip area, would cause a greater loss in lift at the tip of the wing having a taper ratio of 0.25 than at the tip of the wing having a taper ratio

of 0. Thus, greater losses in rolling moment and reduced values of βC_{l_p} would result for the wings having a taper ratio of 0.25.

For the triangular wings (fig. 12), the experimental damping in roll varied from slightly above theory when the leading edges were considerably ahead of the Mach cone to approximately 25 percent below theory when the leading edges were subsonic or in the vicinity of the Mach cone. The results are in fair agreement with the results for triangular wings obtained in references 6 and 7, although in the present investigation the damping in roll for triangular wings with supersonic leading edges was higher than that obtained in references 6 and 7, for $\beta \cot \Lambda > 1.30$. This difference was probably due to the fact that in references 6 and 7 the wings were mounted on a much larger body of revolution than the mounting sting used in the present tests. As $\beta \cot \Lambda$ decreased to low values ($\beta \cot \Lambda < 0.90$), the results of the present tests and those of references 6 and 7 showed a tendency toward closer agreement with theory.

Theoretically the variation of βC_{l_p} with $\beta \cot \Lambda$ may be represented by a single curve independent of Mach number, for swept, tapered wings with common values of βA and λ . (For triangular wings a common value of βA is not required.) Experimentally, a somewhat different curve resulted for each Mach number. (See figs. 8 to 10 and 12.) In general, this occurred to a greater extent when the leading edges were subsonic than when the leading edges were supersonic.

The experimental damping in roll of the two 1/8-inch-thick wings (wings 10-A and 27-A) was different from that of the 3/16-inch-thick wings of very nearly identical plan forms (wings 10 and 27). The difference was more pronounced for the subsonic-leading-edge wings (wings 10 and 10-A) than for the highly supersonic-leading-edge wings (wings 27 and 27-A). For all three Mach numbers (and values of βA), the damping in roll of the thin subsonic-leading-edge wings was higher than that of the corresponding thicker wings - approximately 20 percent higher at $M = 2.41$ ($\beta A \approx 5.00$, fig. 10), 30 percent higher at $M = 1.93$ ($\beta A \approx 4.00$, fig. 9), and 70 percent higher at $M = 1.62$ ($\beta A \approx 3.00$, fig. 8). That is, the values of βC_{l_p} for thin wings were more nearly in agreement with those predicted by theory. This would be expected, since the wings were assumed to have zero thickness in the theoretical calculations.

CONCLUDING REMARKS

Wind-tunnel tests were made at Mach numbers of 1.62, 1.93, and 2.41 of the damping-in-roll derivatives of a series of 33 swept and tapered wings.

The damping in roll appeared to be predicted quite accurately by the linear theory when the wing leading edges were well ahead of the Mach cones emanating from the wing apices. When the leading edges were in the vicinity of or behind the Mach cones, the experimental damping in roll was considerably less than that predicted by theory. Poorer agreement with theory was obtained for the wings having a taper ratio of 0.25 with leading edges behind or in the vicinity of the Mach cone than for the wings having a taper ratio of 0 with the same leading-edge positions relative to the Mach cone.

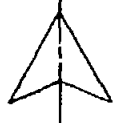
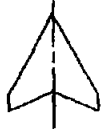
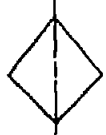
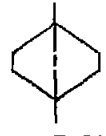
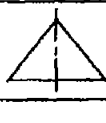
It was found that the damping in roll of the thin wings agreed more closely with theory than that of the thicker wings of identical plan forms. The difference in the damping in roll for the wings of different thicknesses but identical plan forms was greater when the leading edges were behind the Mach cone than when the leading edges were ahead of the Mach cone.

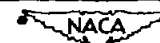
Langley Aeronautical Laboratory,
National Advisory Committee for Aeronautics,
Langley Field, Va.

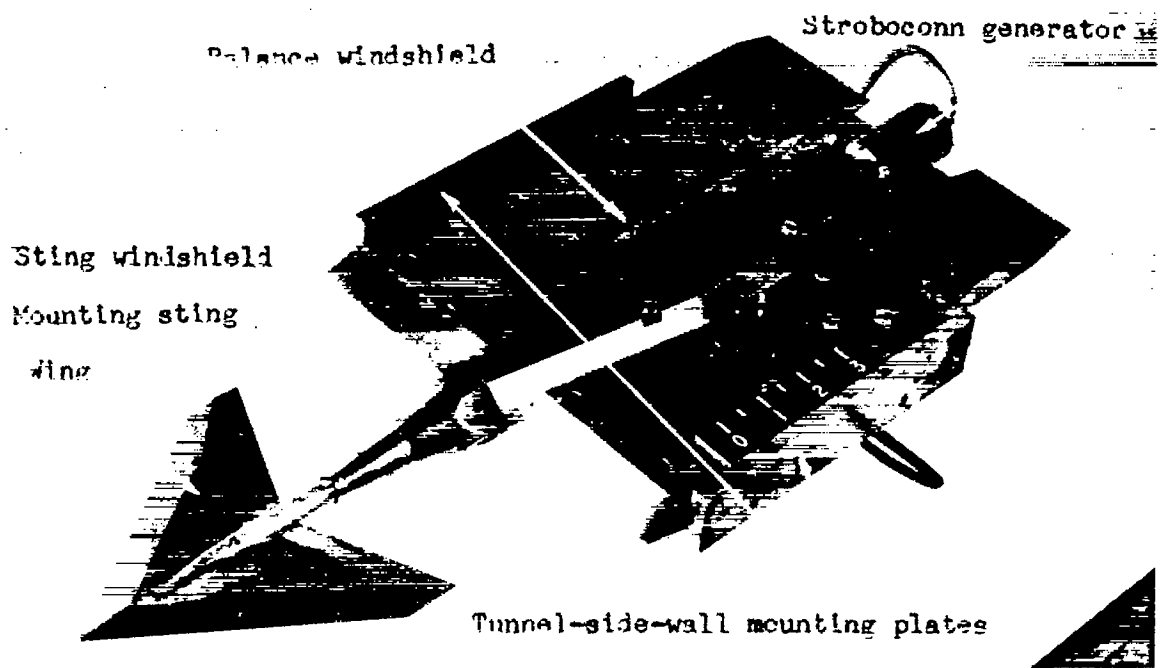
REFERENCES

1. Harmon, Sidney M., and Jeffreys, Isabella: Theoretical Lift and Damping in Roll of Thin Wings With Arbitrary Sweep and Taper at Supersonic Speeds. Supersonic Leading and Trailing Edges. NACA TN 2114, 1950.
2. Malvestuto, Frank S., Jr., Margolis, Kenneth, and Ribner, Herbert S.: Theoretical Lift and Damping in Roll at Supersonic Speeds of Thin Sweptback Tapered Wings With Streamwise Tips, Subsonic Leading Edges, and Supersonic Trailing Edges. NACA Rep. 970, 1950. (Supersedes NACA TN 1860.)
3. Ribner, Herbert S.: On the Effect of Subsonic Trailing Edges on Damping in Roll and Pitch of Thin Sweptback Wings in a Supersonic Stream. NACA TN 2146, 1950.
4. Brown, Clinton E., and Adams, Mac C.: Damping in Pitch and Roll of Triangular Wings at Supersonic Speeds. NACA Rep. 892, 1948. (Supersedes NACA TN 1566.)
5. Piland, Robert O.: Summary of the Theoretical Lift, Damping-In-Roll, and Center-of-Pressure Characteristics of Various Wing Plan Forms at Supersonic Speeds. NACA TN 1977, 1949.
6. Brown, Clinton E., and Heinke, Harry S., Jr.: Preliminary Wind-Tunnel Tests of Triangular and Rectangular Wings in Steady Roll at Mach Numbers of 1.62 and 1.92. NACA RM 18130, 1949.
7. Bland, William M., Jr., and Sandahl, Carl A.: A Technique Utilizing Rocket-Propelled Test Vehicles for the Measurement of the Damping in Roll of Sting-Mounted Models and Some Initial Results for Delta and Unswept Tapered Wings. NACA RM 150D24, 1950.
8. Sanders, E. Claude, Jr.: Damping in Roll of Models With 45°, 60°, and 70° Delta Wings Determined at High Subsonic, Transonic, and Supersonic Speeds With Rocket-Powered Models. NACA RM 152D22a, 1952.
9. Bland, William M., Jr.: Effect of Fuselage Interference on the Damping in Roll of Delta Wings of Aspect Ratio 4 in the Mach Number Range Between 0.6 and 1.6 As Determined With Rocket-Propelled Vehicles. NACA RM 152E13, 1952.
10. Hopko, Russell N.: A Flight Investigation of the Damping in Roll and Rolling Effectiveness Including Aeroelastic Effects of Rocket-Propelled Missile Models Having Cruciform, Triangular, Interdigitated Wings and Tails. NACA RM 151D16, 1951.

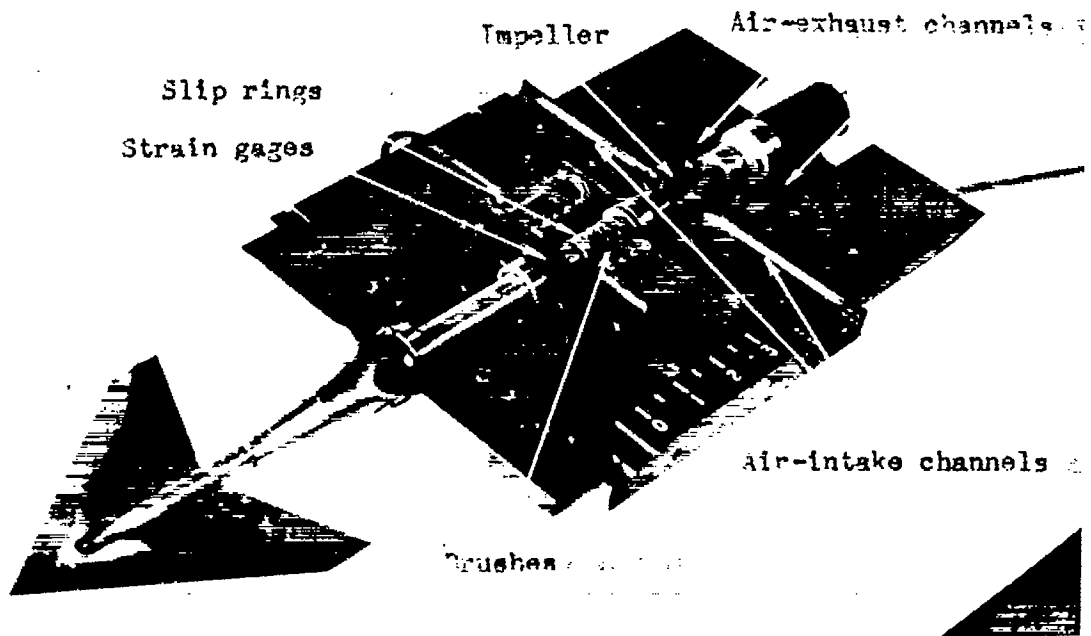
TABLE I. - WING DIMENSIONS AND PARAMETERS

Plan form	Wing	Λ (deg.)	Λ_{TE} (deg.)	b (ft.)	t (ft.)	c_r (ft.)	λ	S (sq.ft.)	A	βA		
										M=1.62	M=1.93	M=2.41
	1	70.0	29.2	0.416	0.0156	0.457	0	0.095	1.82	2.32	3.01	4.00
	2	69.9	45.4	.417	.0156	.357	0	.074	2.34	2.98	3.86	5.12
	3	65.0	23.1	.416	.0156	.357	0	.074	2.33	2.97	3.85	5.12
	4	65.0	40.0	.496	.0156	.324	0	.080	3.06	3.90	5.06	6.72
	5	60.0	23.2	.580	.0156	.378	0	.110	3.07	3.92	5.07	6.74
	6	70.0	54.7	.375	.0156	.326	.25	.075	1.87	2.38	3.08	4.10
	7	64.7	39.6	.375	.0156	.325	.25	.077	1.84	2.34	3.04	4.03
	8	60.0	22.3	.500	.0156	.428	.25	.131	1.90	2.43	3.14	4.18
	9	55.0	8.0	.500	.0156	.423	.25	.131	1.91	2.43	3.15	4.19
	10	69.8	59.5	.396	.0156	.271	.25	.067	2.34	2.98	3.87	5.14
	10-A	70.0	59.4	.396	.0104	.271	.25	.066	2.37	3.02	3.92	5.20
	11	65.0	47.8	.398	.0156	.273	.25	.068	2.34	2.99	3.87	5.14
	12	55.0	22.0	.500	.0156	.339	.25	.106	2.37	3.02	3.91	5.19
	13	65.1	53.7	.459	.0156	.242	.25	.069	3.06	3.90	5.06	6.72
	14	60.0	43.2	.542	.0156	.281	.25	.094	3.12	3.97	5.15	6.84
	15	55.2	33.1	.542	.0156	.275	.25	.091	3.22	4.11	5.32	7.07
	16	45.0	12.9	.542	.0156	.279	.25	.094	3.12	3.98	5.15	6.84
	17	55.0	-37.2	.524	.0156	.574	0	.151	1.83	2.33	3.02	4.01
	18	50.0	-45.1	.530	.0156	.582	0	.154	1.82	2.32	3.01	3.99
	19	47.4	-47.6	.530	.0156	.579	0	.153	1.83	2.34	3.03	4.02
	20	54.9	-16.2	.581	.0156	.497	0	.145	2.34	2.98	3.86	5.12
	21	45.0	-36.1	.576	.0156	.498	0	.144	2.31	2.95	3.82	5.08
	22	40.4	-40.6	.568	.0156	.485	0	.138	2.34	2.98	3.87	5.14
	23	45.0	-16.9	.579	.0156	.378	0	.110	3.07	3.91	5.06	6.72
	24	33.4	-33.6	.566	.0156	.375	0	.106	3.02	3.85	4.99	6.63
	25	33.5	-33.6	.500	.0156	.431	.25	.133	1.88	2.41	3.11	4.13
	26	45.0	-1.8	.500	.0156	.344	.25	.107	2.33	2.97	3.85	5.12
	27	27.3	-27.5	.500	.0156	.338	.25	.104	2.41	3.07	3.97	5.28
	27-A	27.4	-27.5	.500	.0104	.341	.25	.106	2.37	3.02	3.92	5.20
	28	21.2	-21.7	.542	.0156	.275	.25	.091	3.22	4.10	5.31	7.06
	29	60.0	-00.2	.582	.0156	.502	0	.146	2.32	2.96	3.83	5.09
	30	55.0	0	.552	.0156	.393	0	.109	2.81	3.58	4.63	6.16
	31	50.0	-0.7	.561	.0156	.330	0	.093	3.40	4.33	5.61	7.45





(a) Completely assembled.



(b) Half of balance windshield removed.

Figure 1.- Photographs of the damping-in-roll test apparatus.

 NACA
L-77911

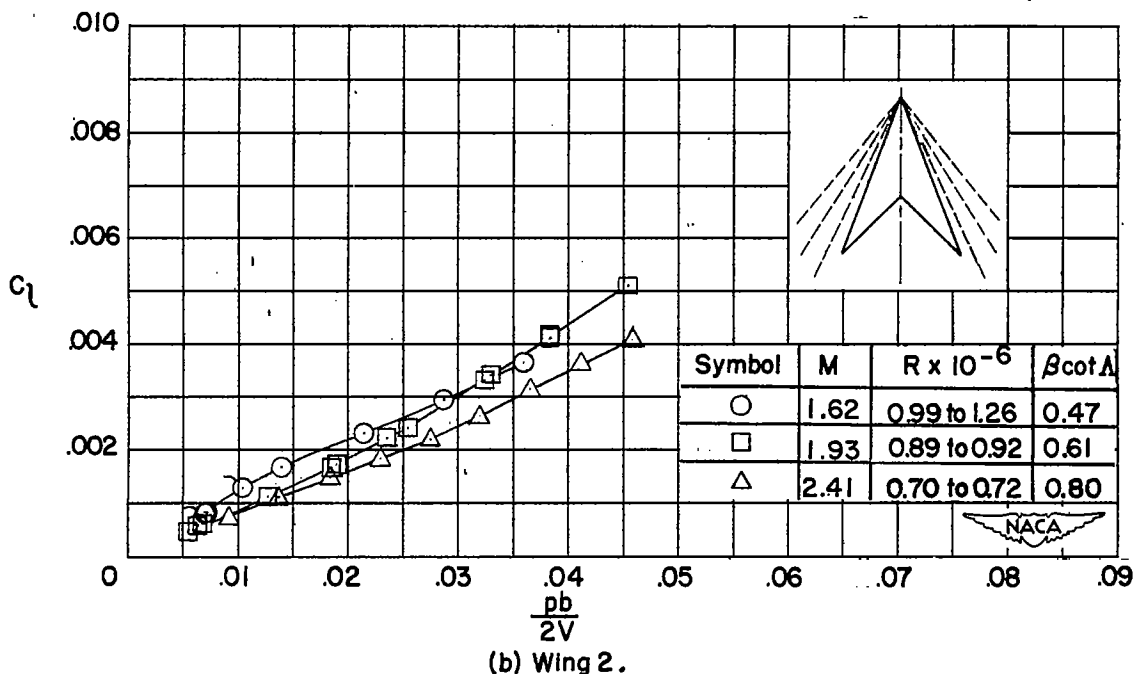
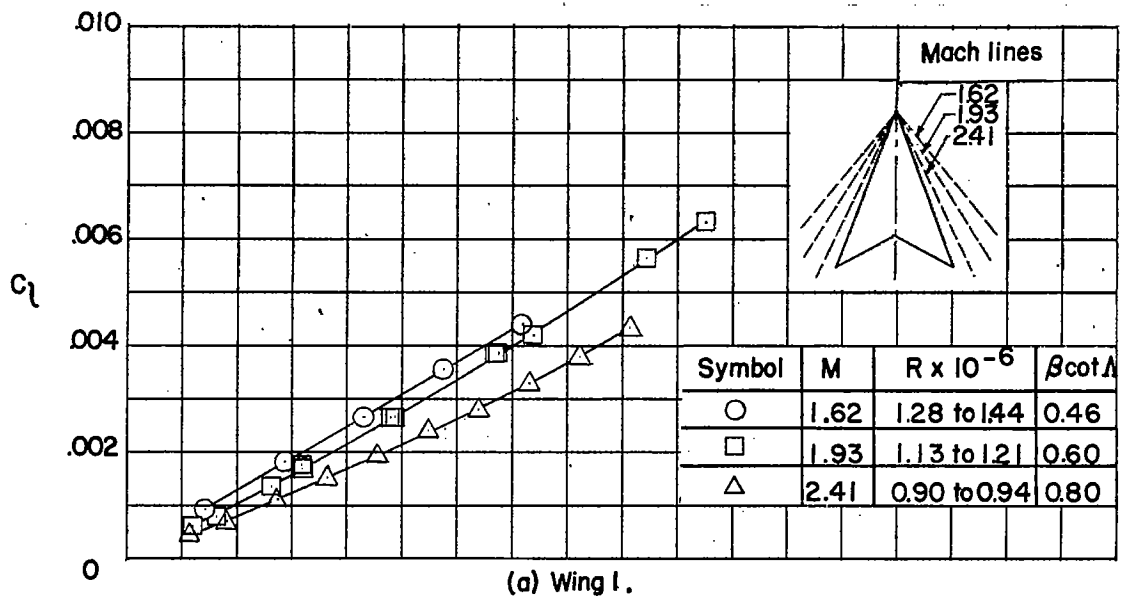
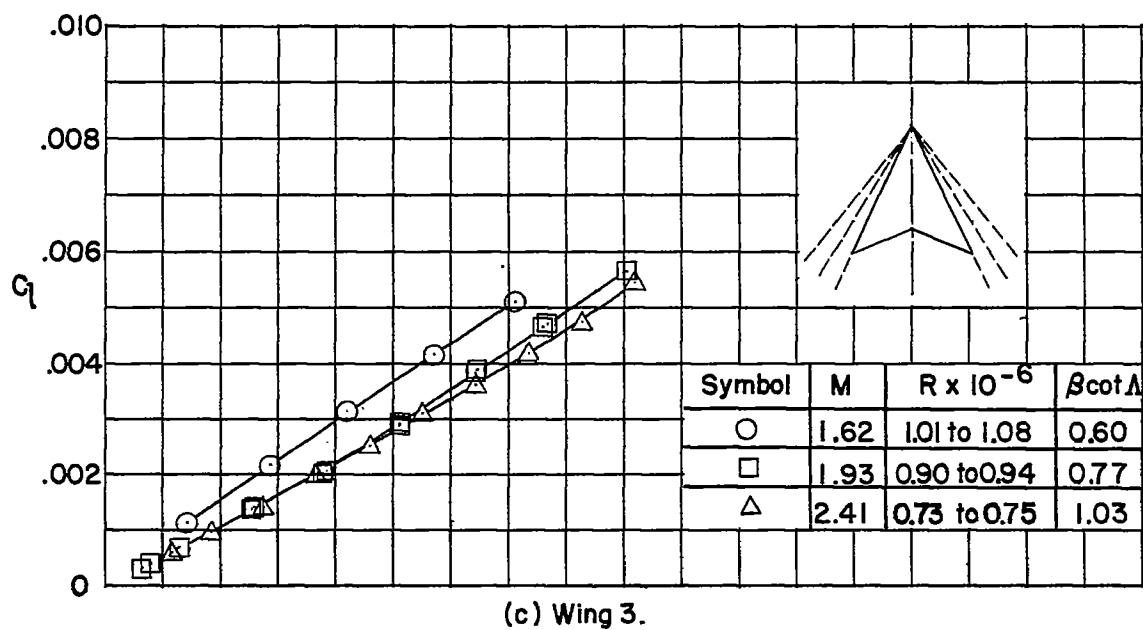
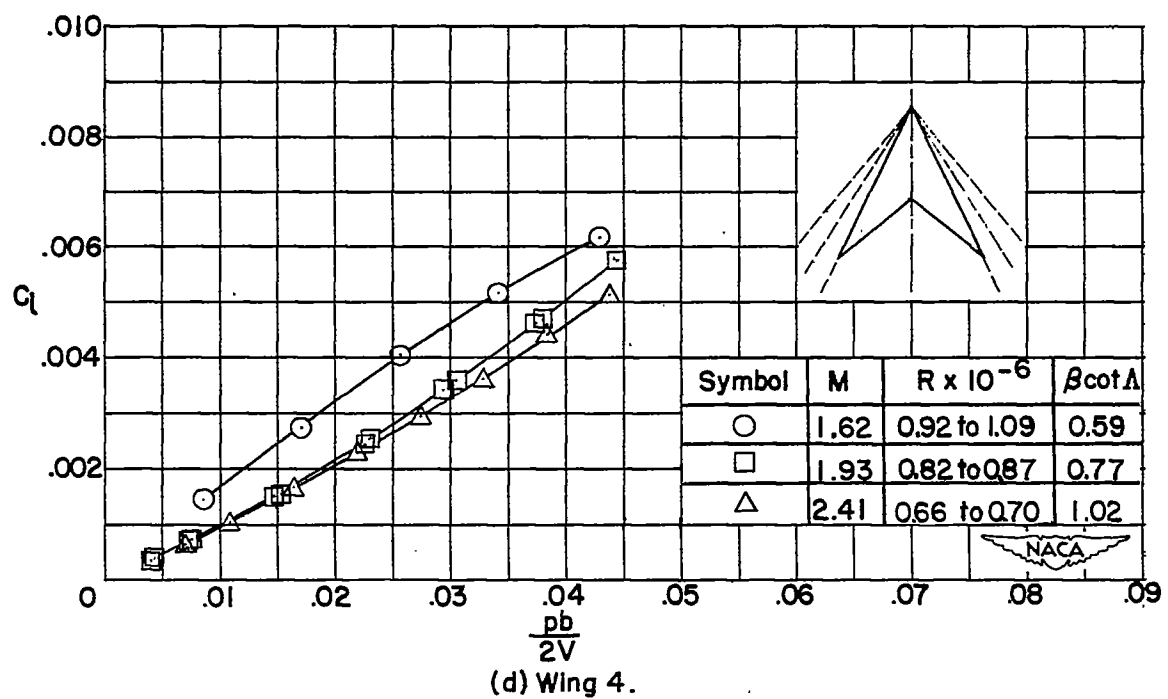


Figure 2.- Variation of rolling-moment coefficient with wing-tip helix angle for wings with sweptback leading and trailing edges, $\lambda = 0$. Flagged symbols indicate check points.



(c) Wing 3.



(d) Wing 4.

Figure 2.- Continued.

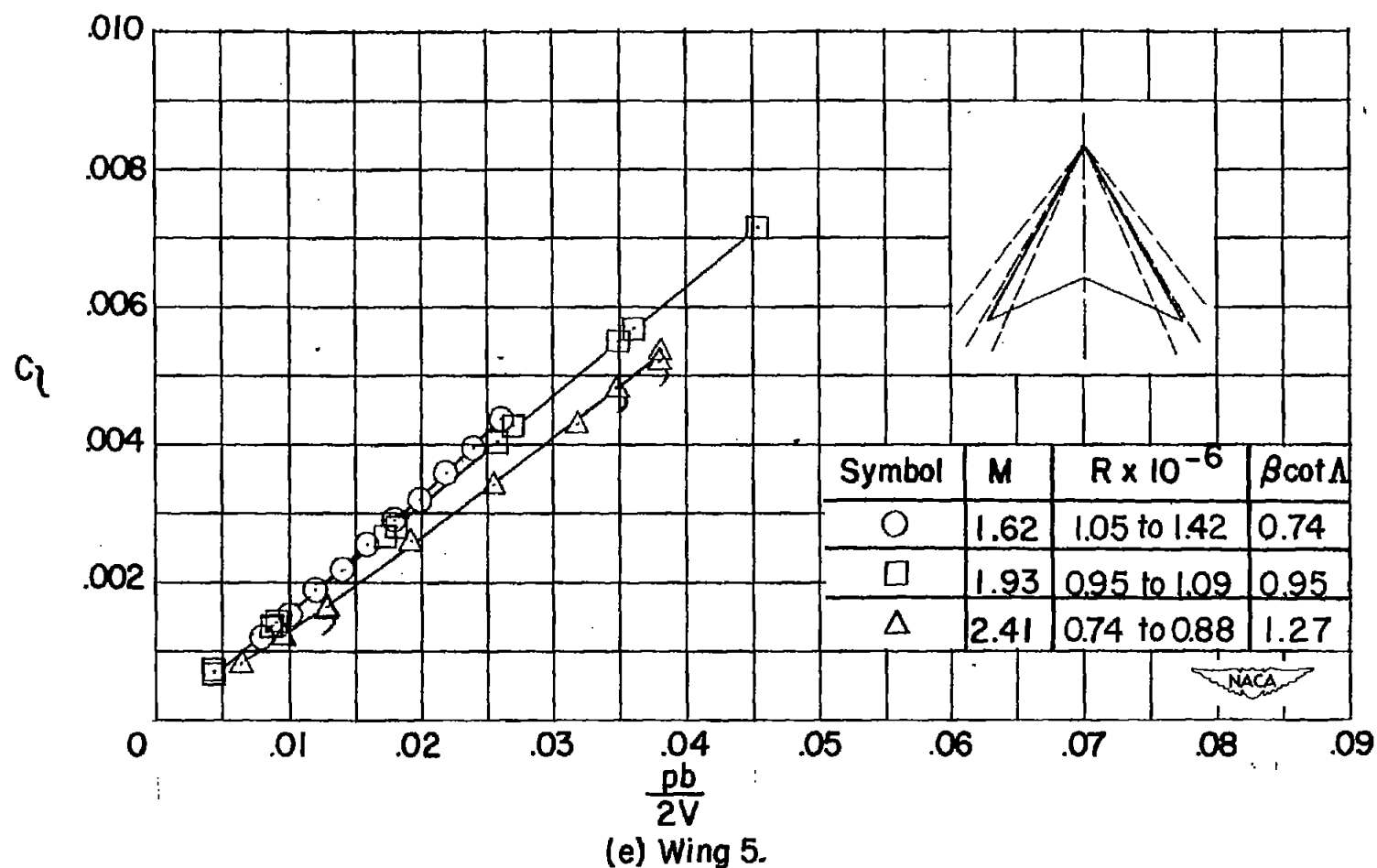


Figure 2.- Concluded.

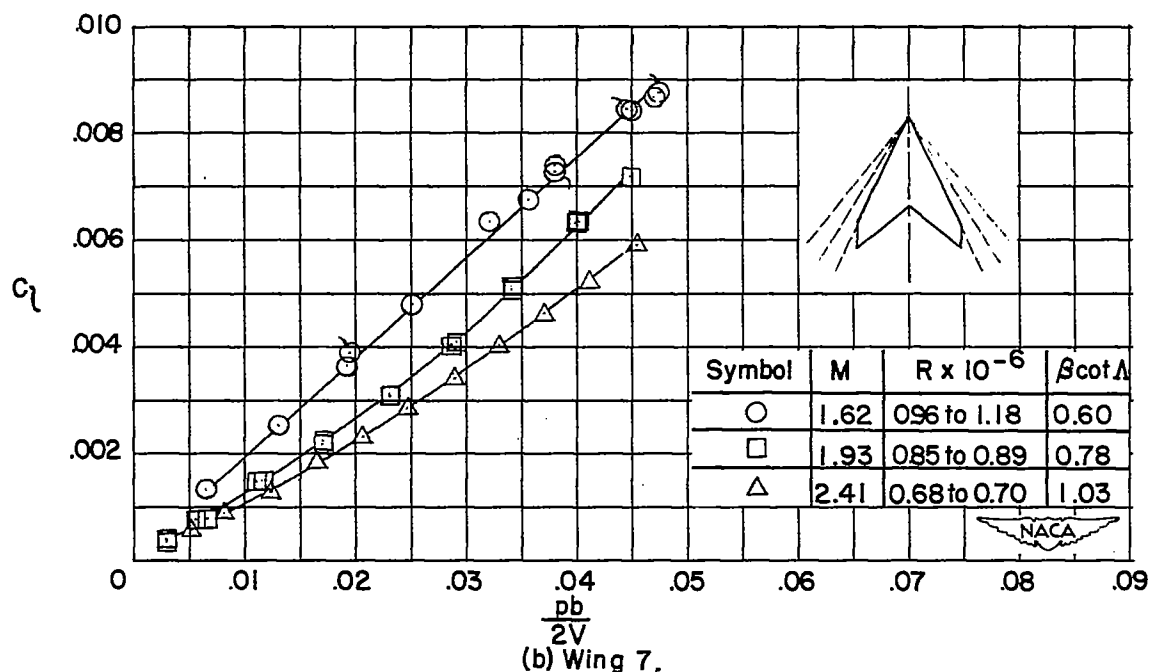
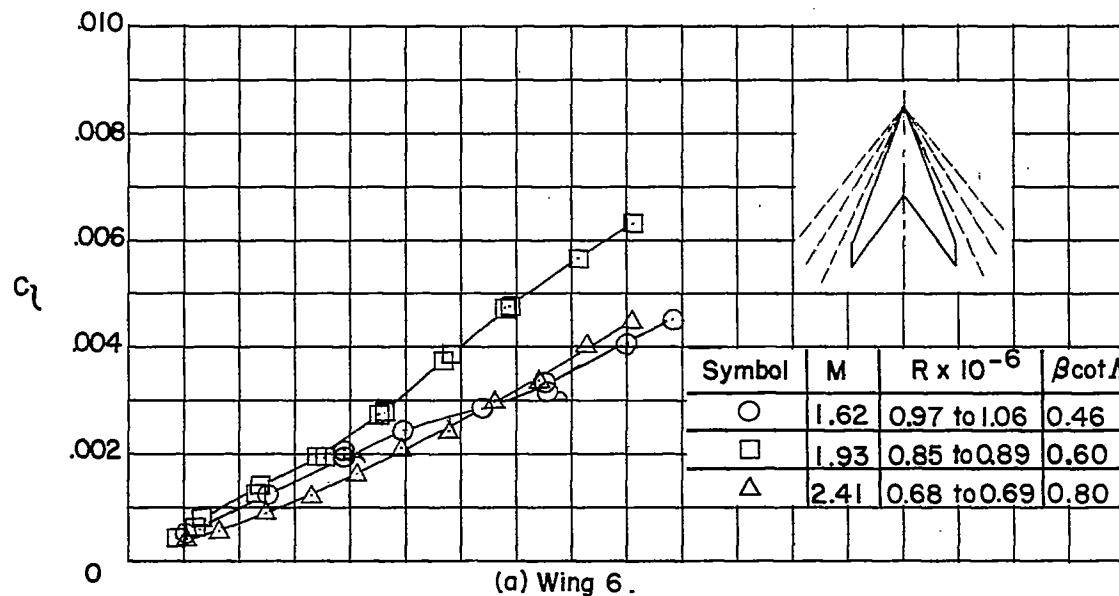
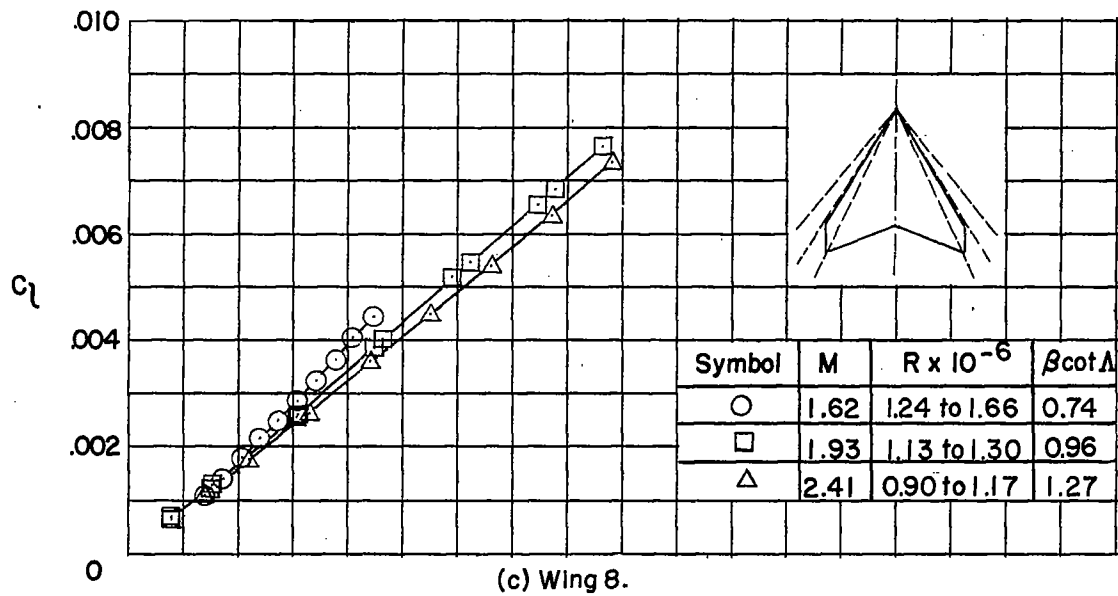
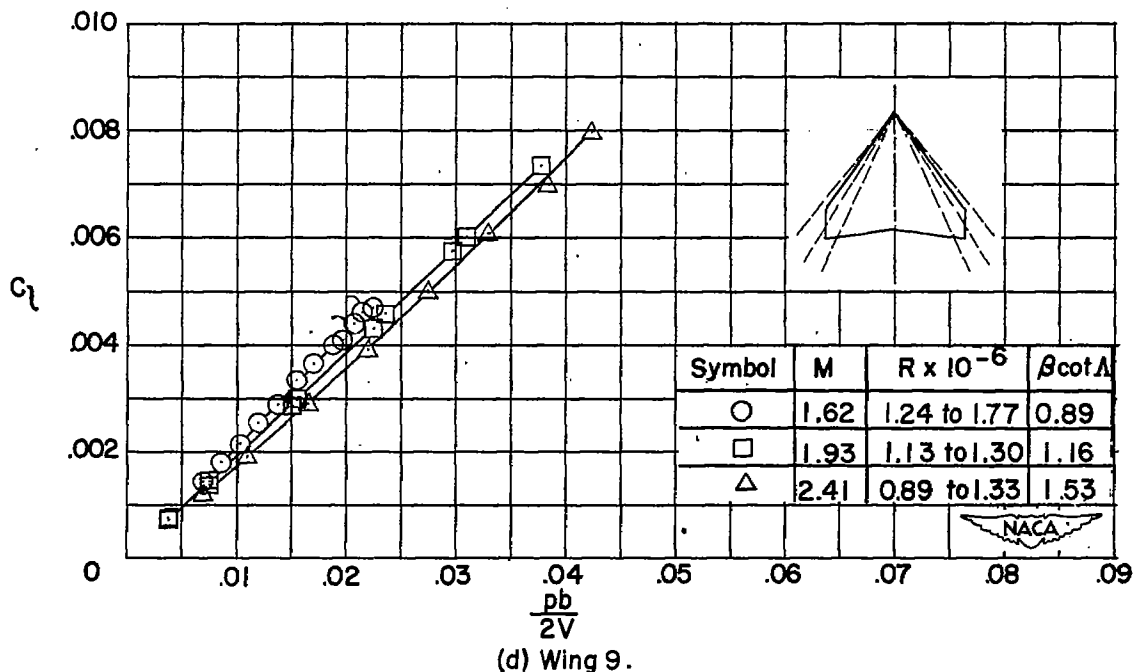


Figure 3.- Variation of rolling-moment coefficient with wing-tip helix angle for wings with sweptback leading and trailing edges, $\lambda = 0.25$. Flagged symbols indicate check points.

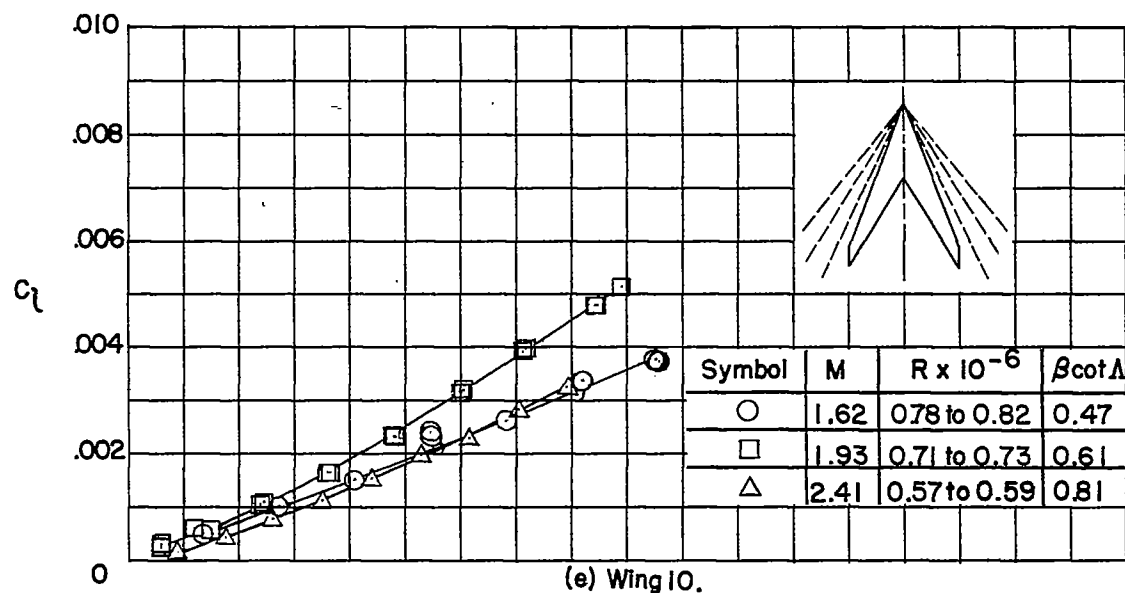


(c) Wing 8.

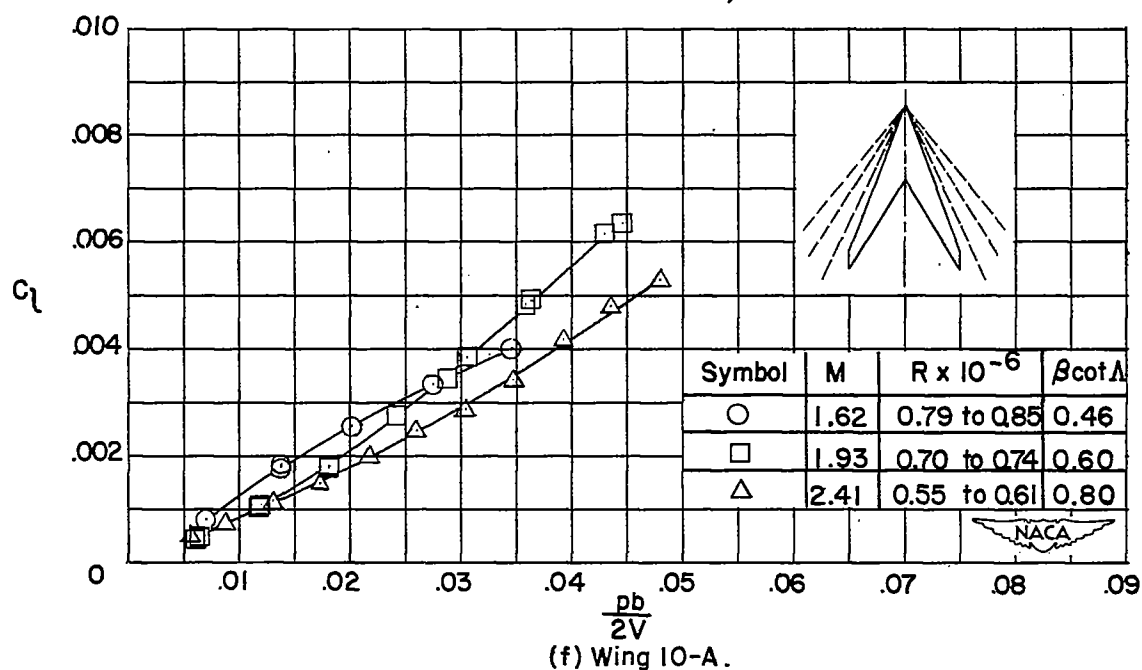


(d) Wing 9.

Figure 3.- Continued.



(e) Wing 10.



(f) Wing 10-A.

Figure 3.- Continued.

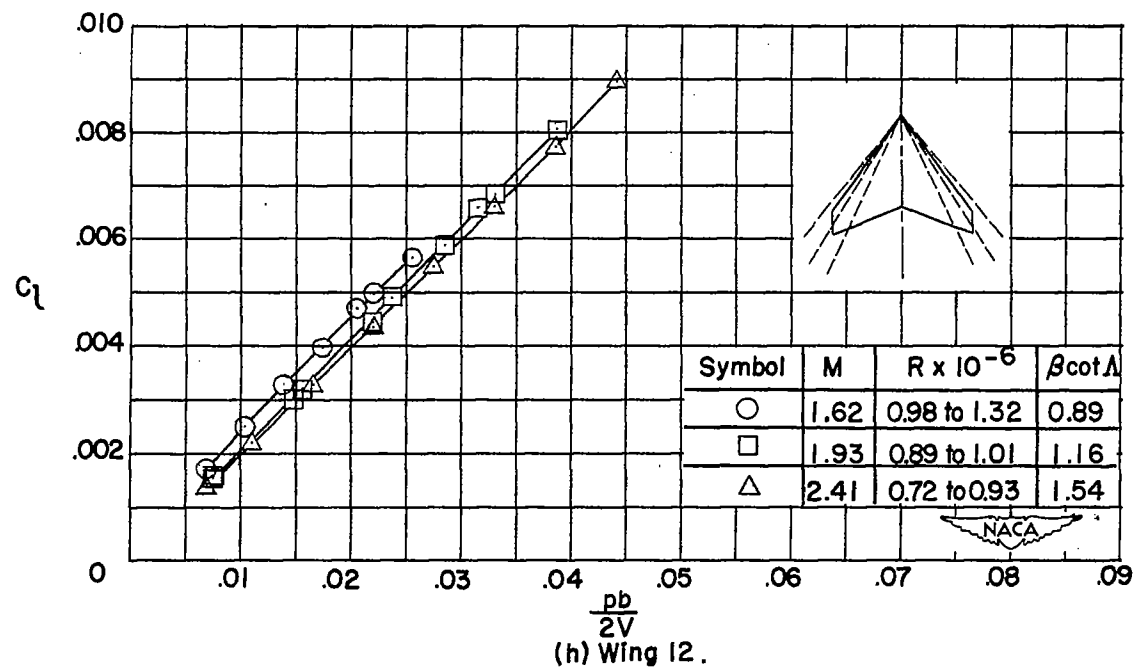
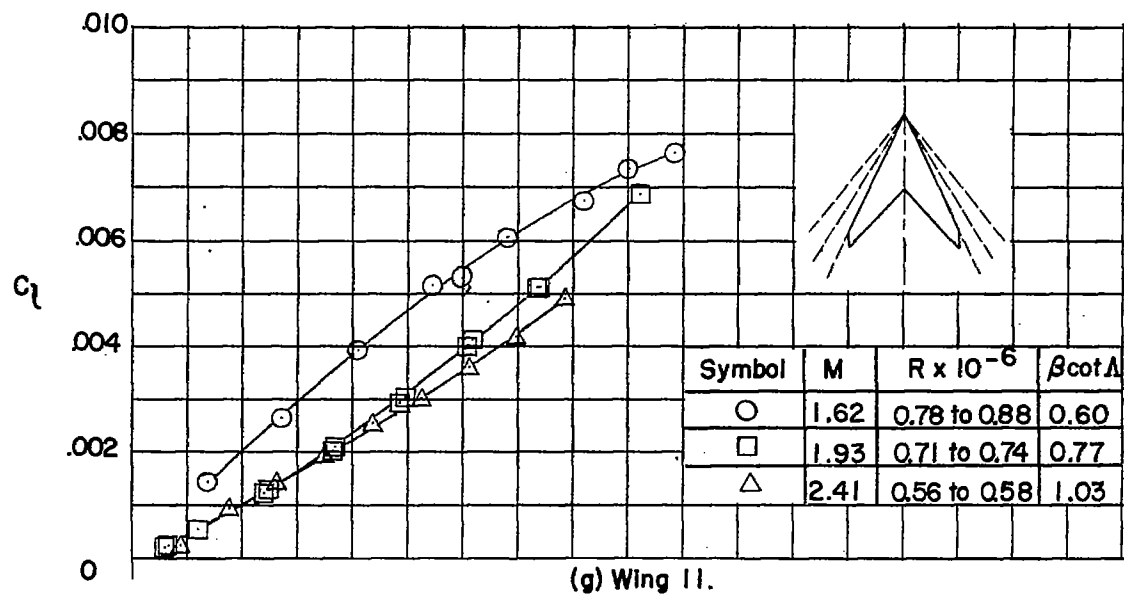


Figure 3.- Continued.

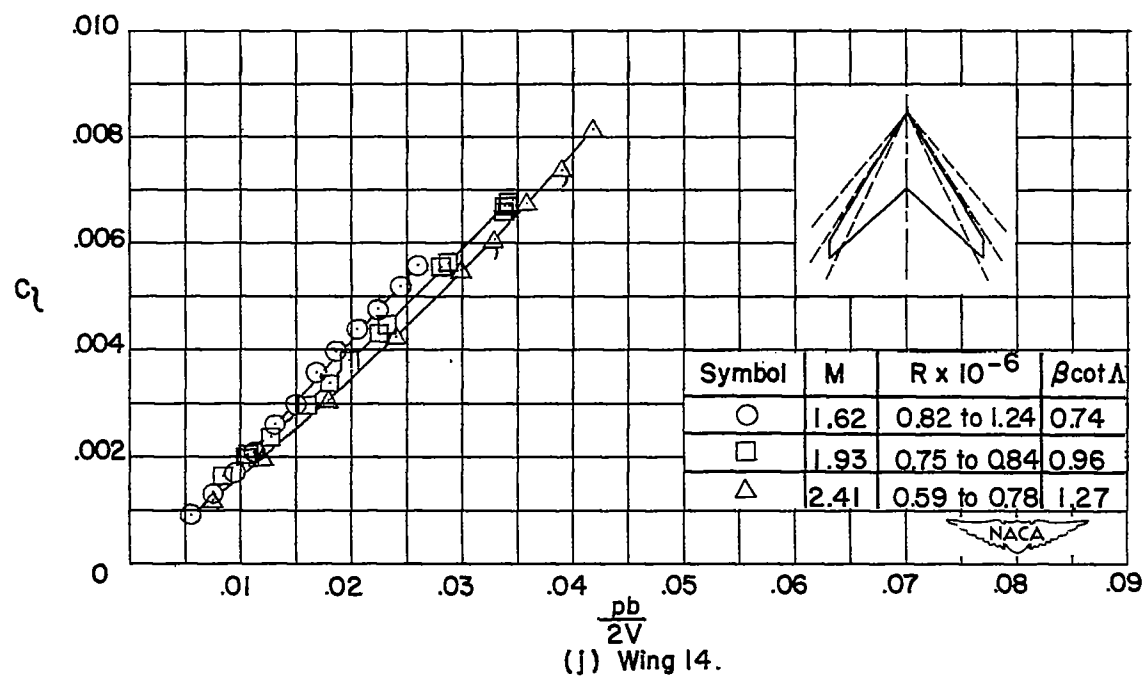
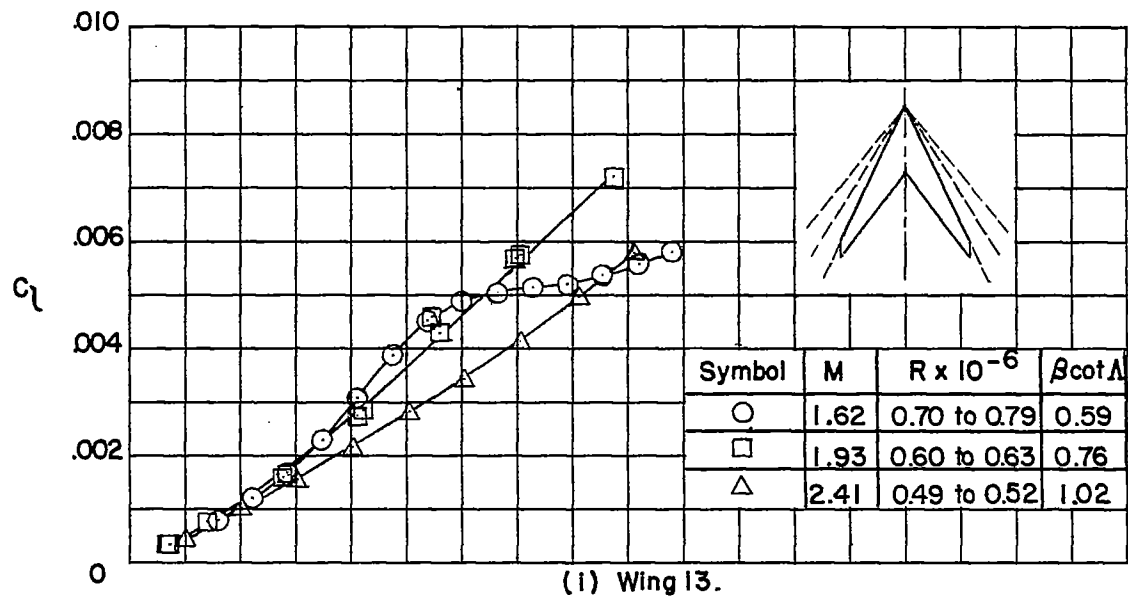
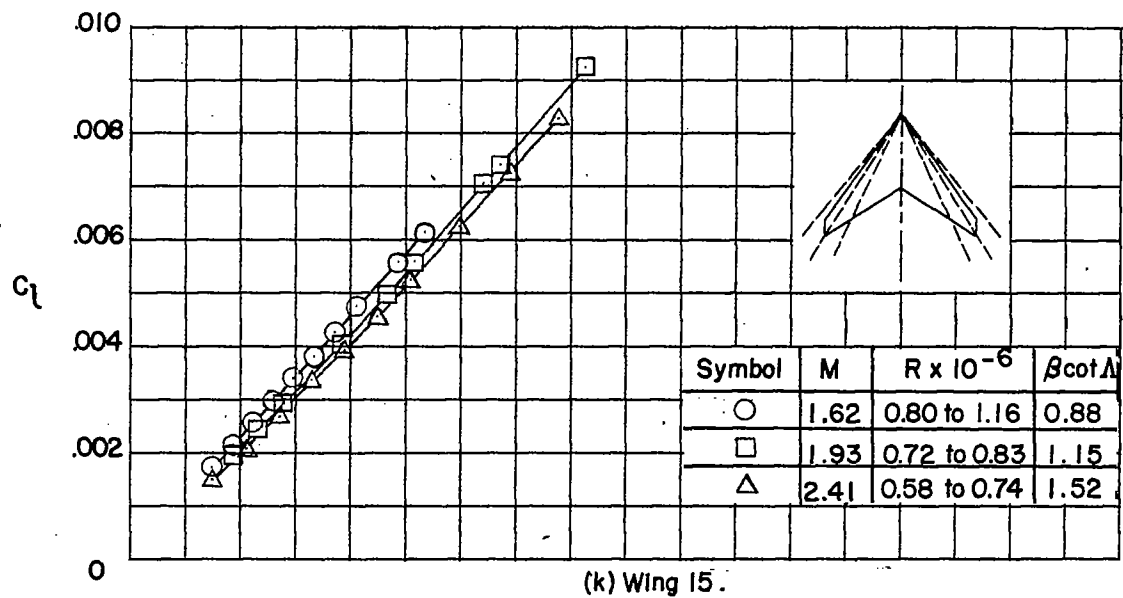
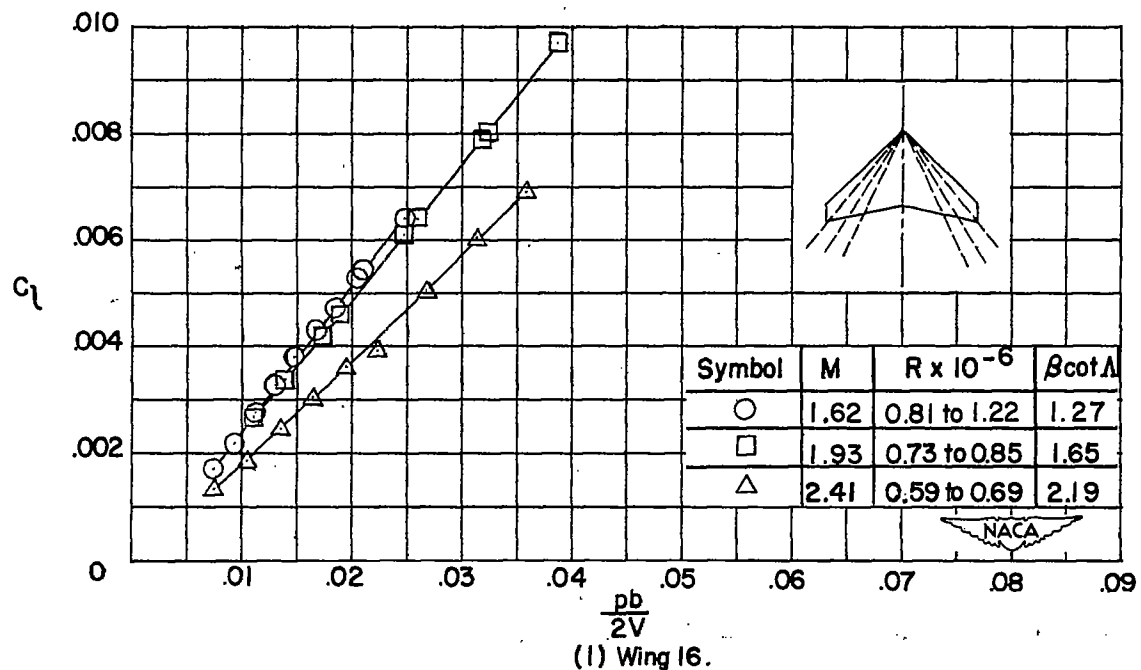


Figure 3.- Continued.

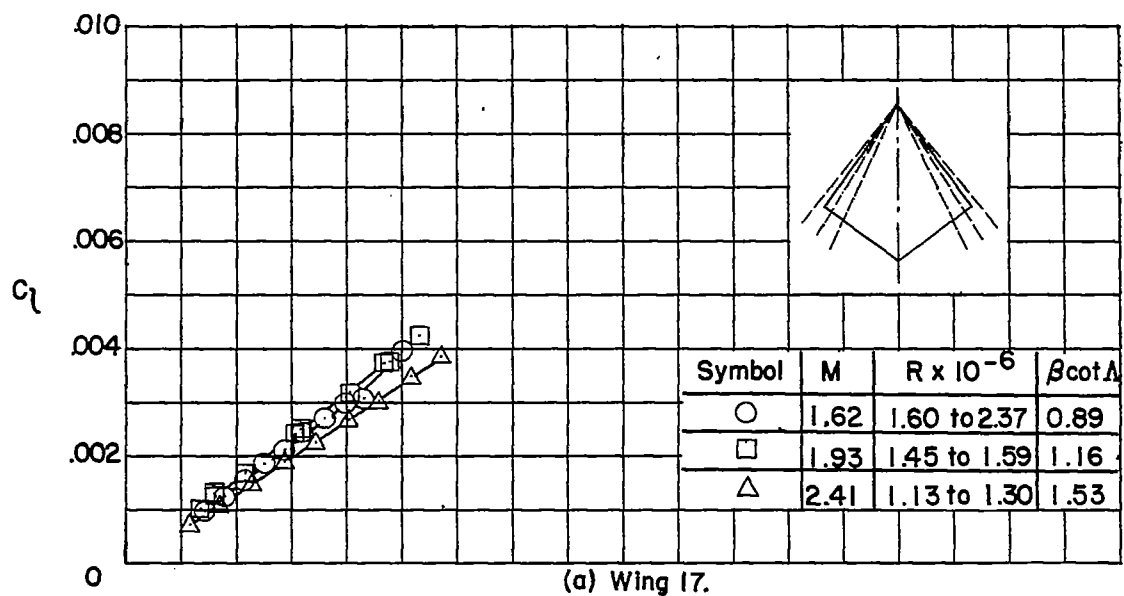


(k) Wing 15.

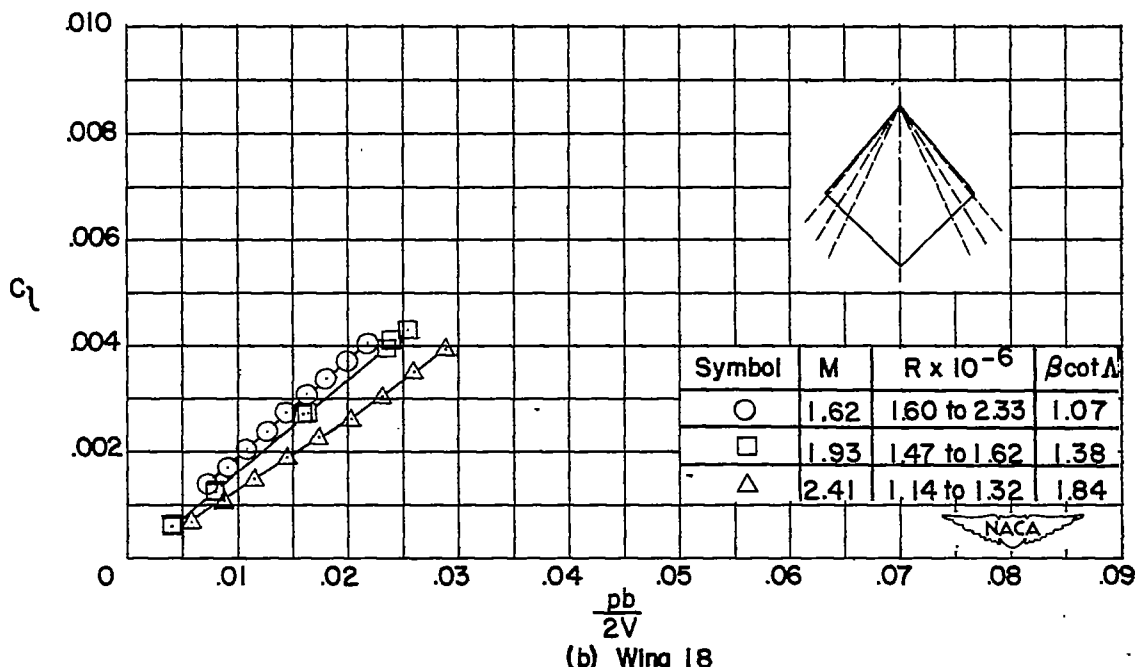


(l) Wing 16.

Figure 3.- Concluded.

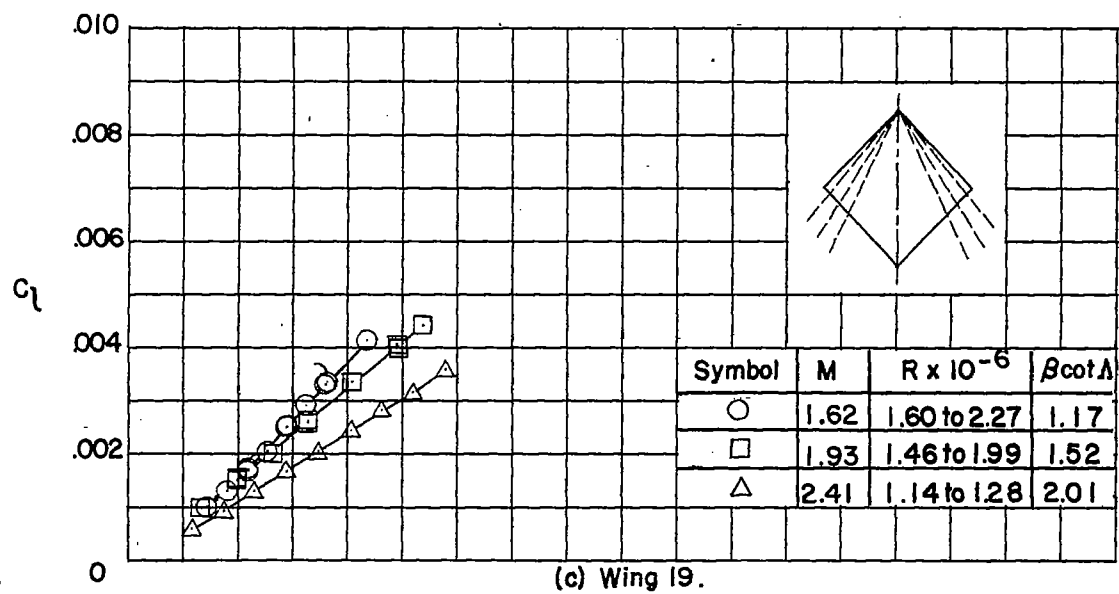


(a) Wing 17.

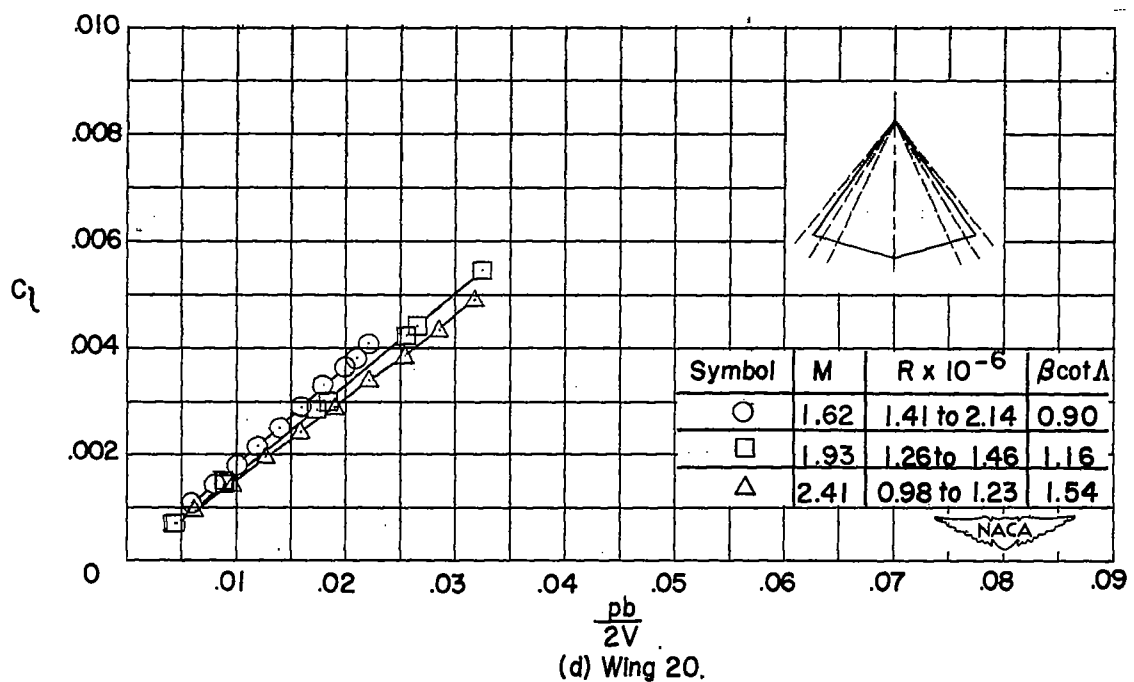


(b) Wing 18.

Figure 4.- Variation of rolling-moment coefficient with wing-tip helix angle for wings with sweptback leading edges and sweptforward trailing edges, $\lambda = 0$. Flagged symbols indicate check points.



(c) Wing 19.



(d) Wing 20.

Figure 4.- Continued.

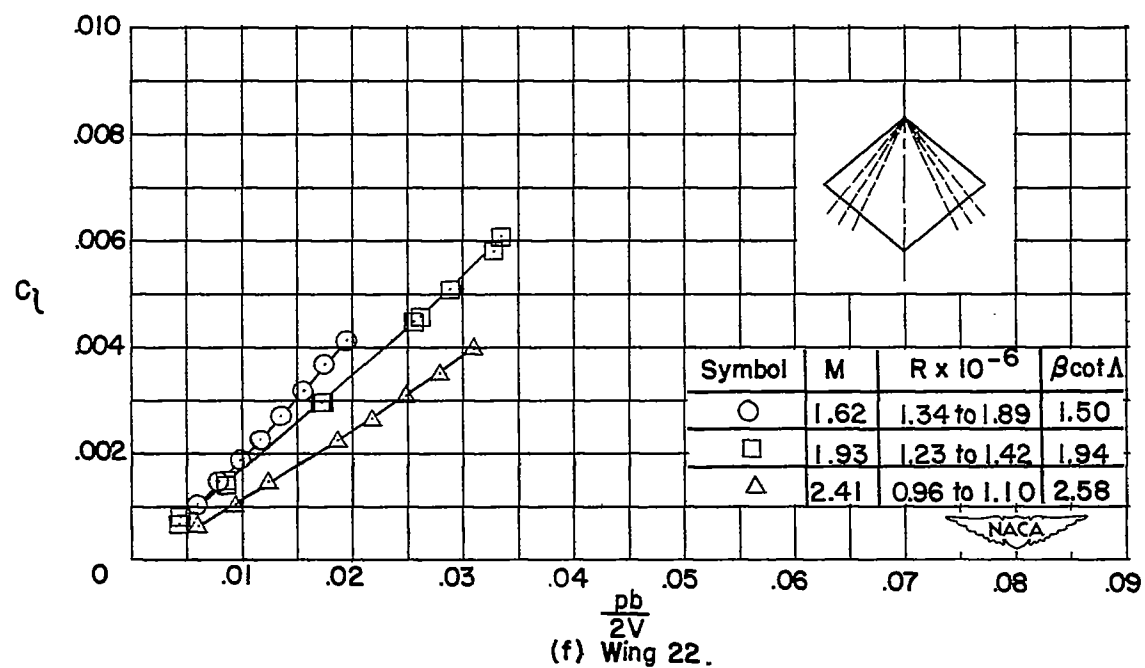
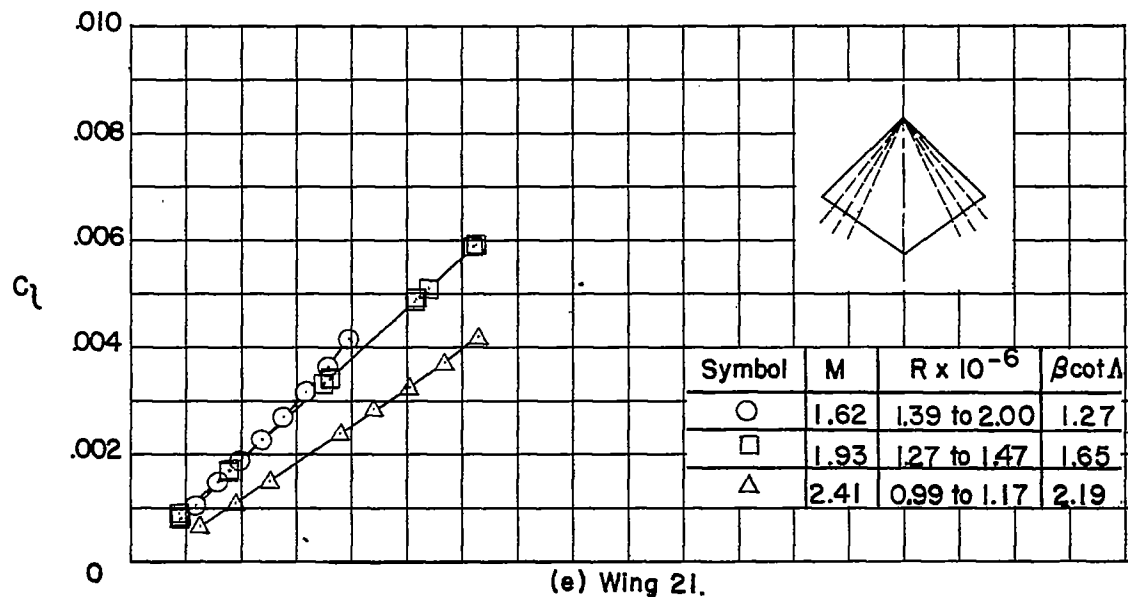


Figure 4.- Continued.

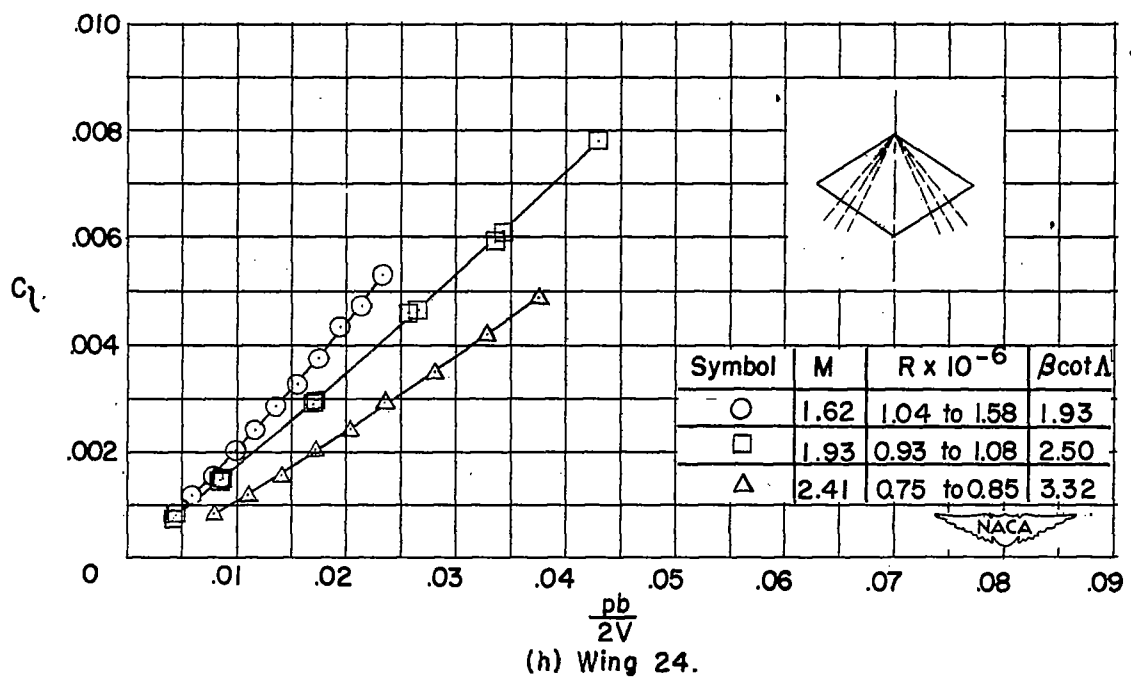
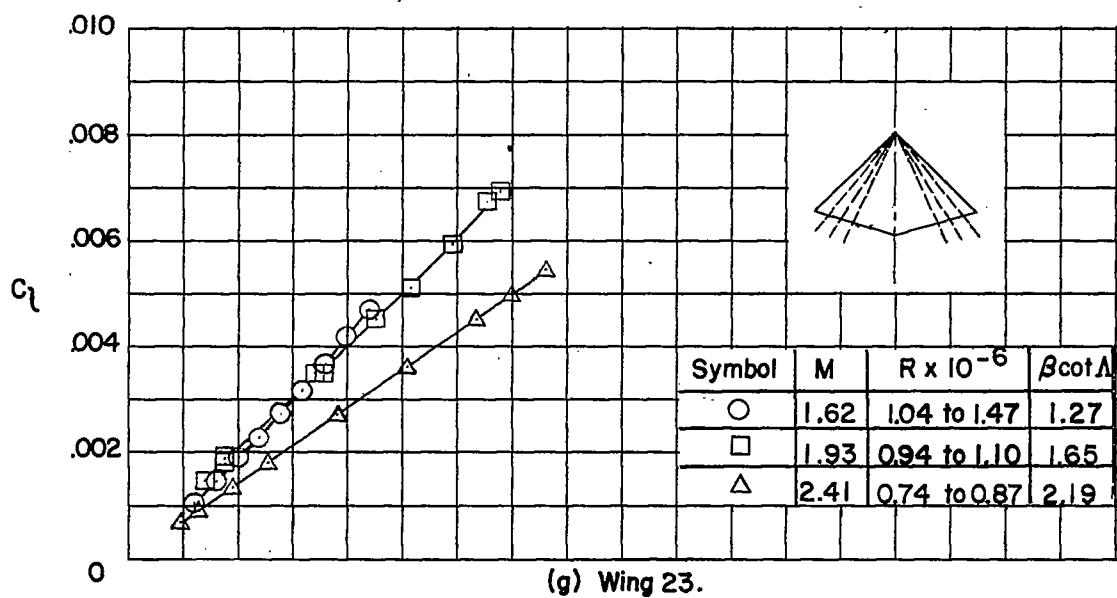
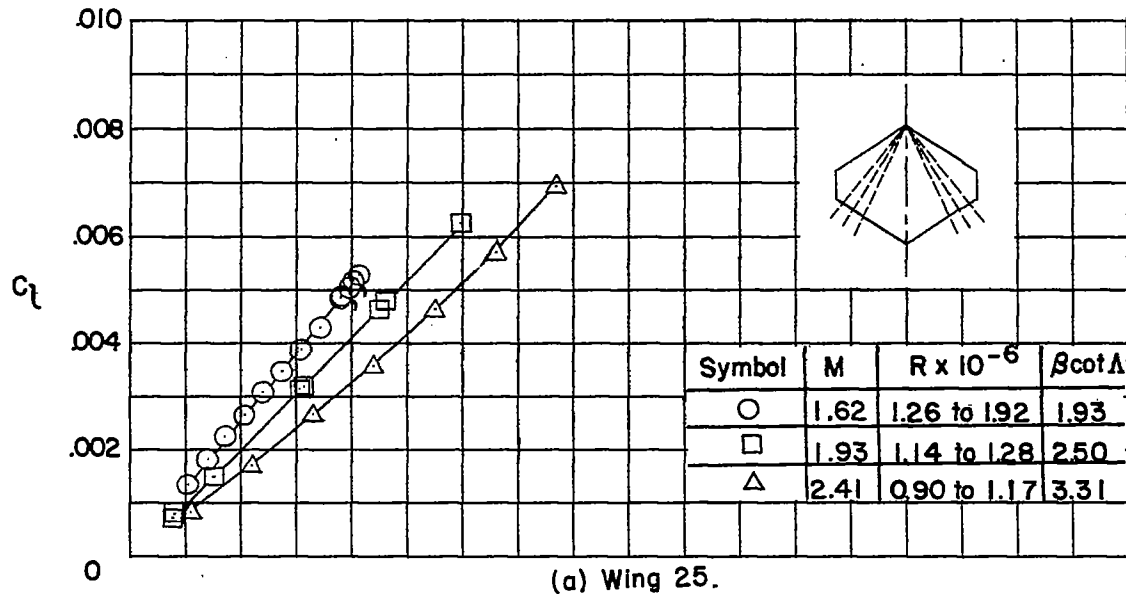
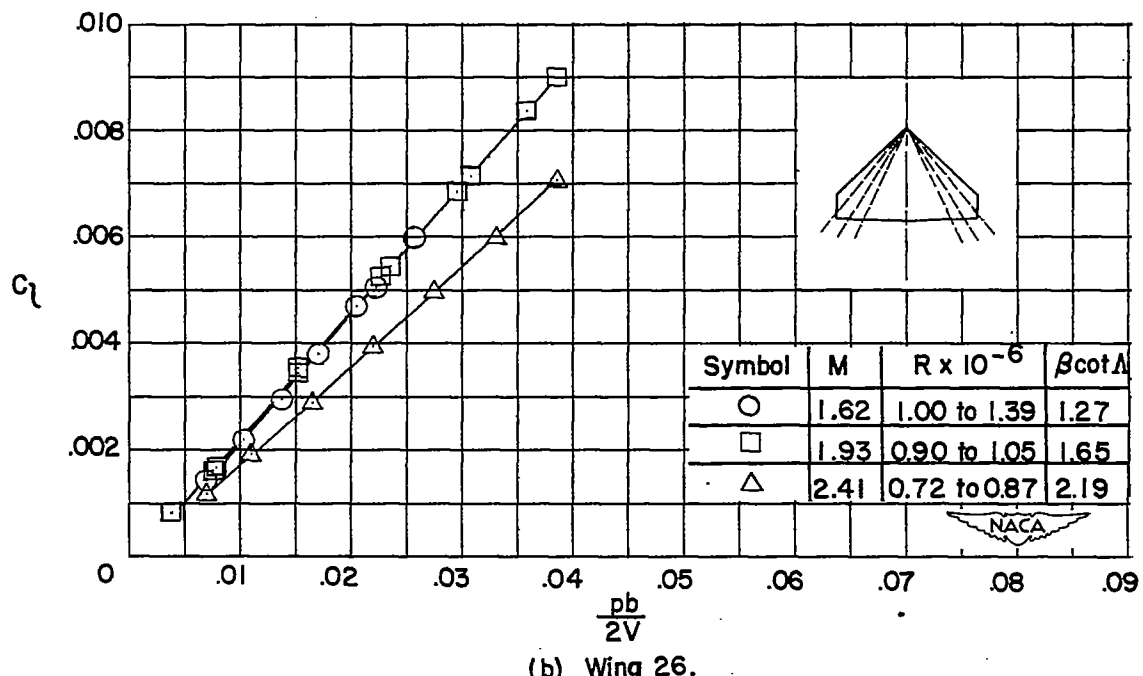


Figure 4.- Concluded.



(a) Wing 25.



(b) Wing 26.

Figure 5.- Variation of rolling-moment coefficient with wing-tip helix angle for wings with sweptback leading edges and sweptforward trailing edges, $\lambda = 0.25$. Flagged symbols indicate check points.

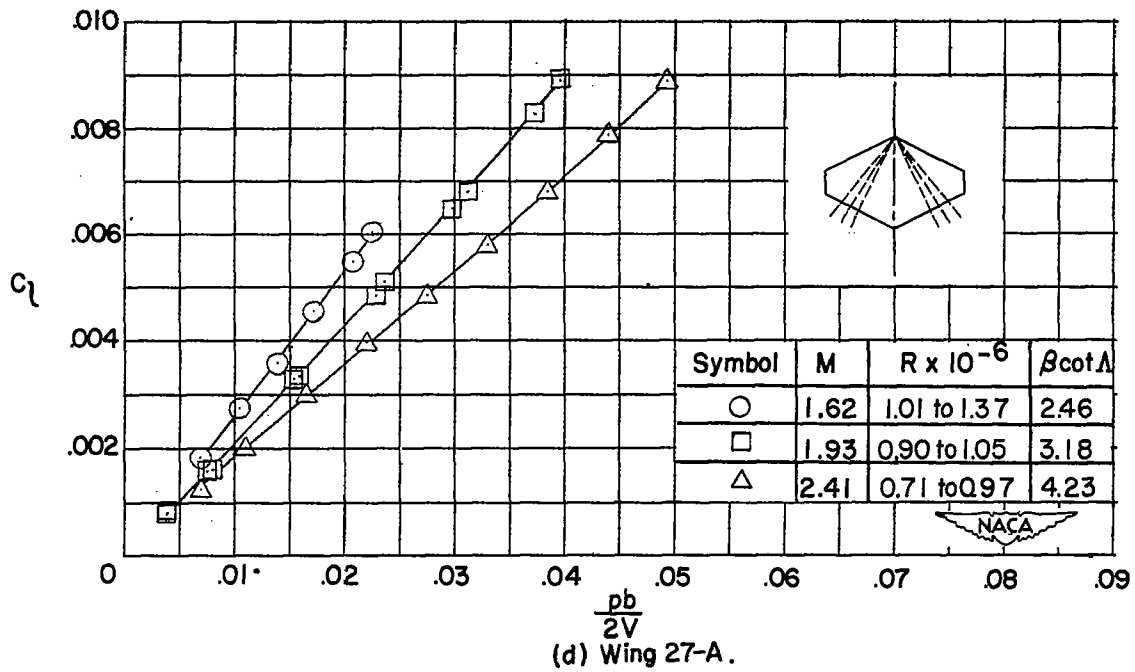
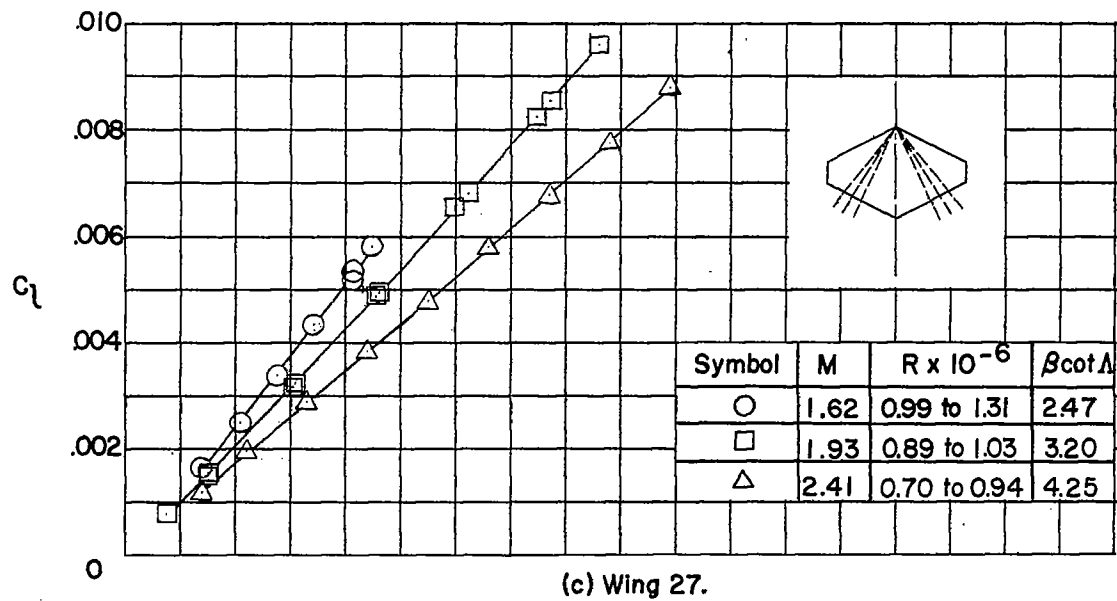


Figure 5.- Continued.

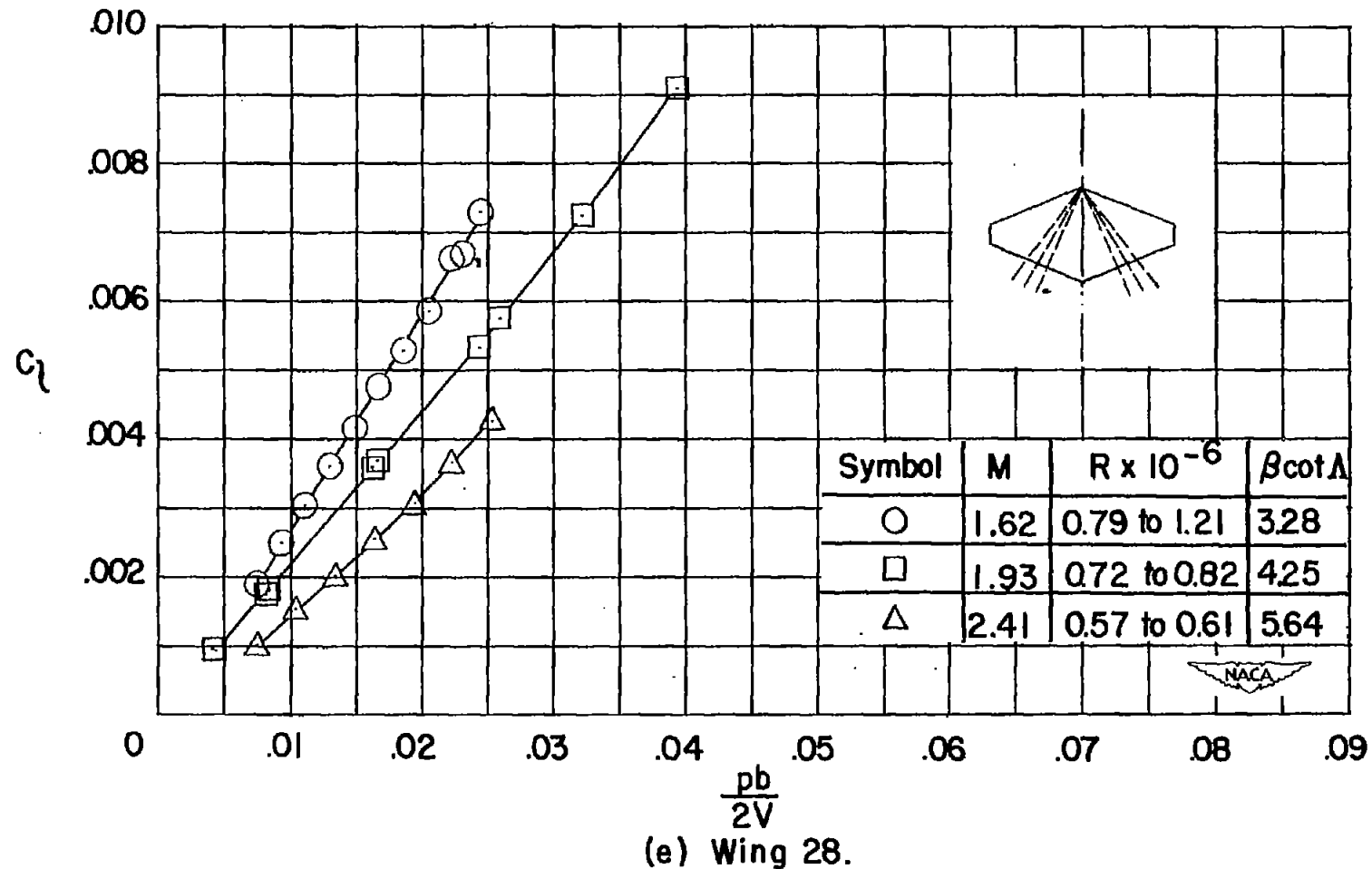


Figure 5.-- Concluded.

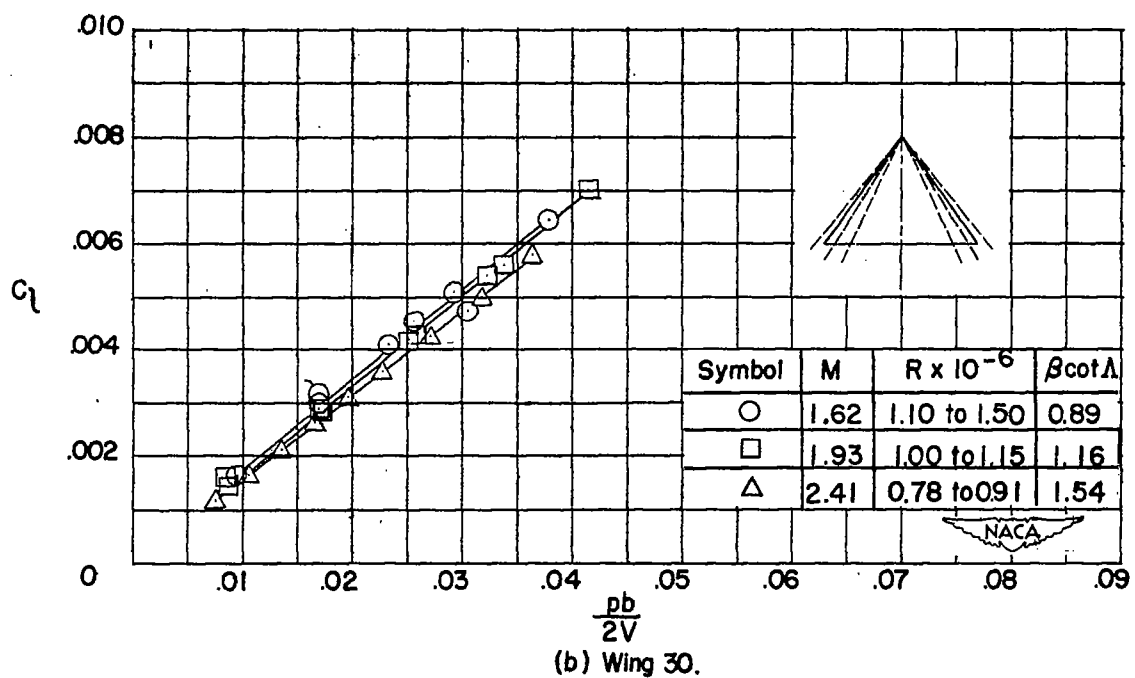
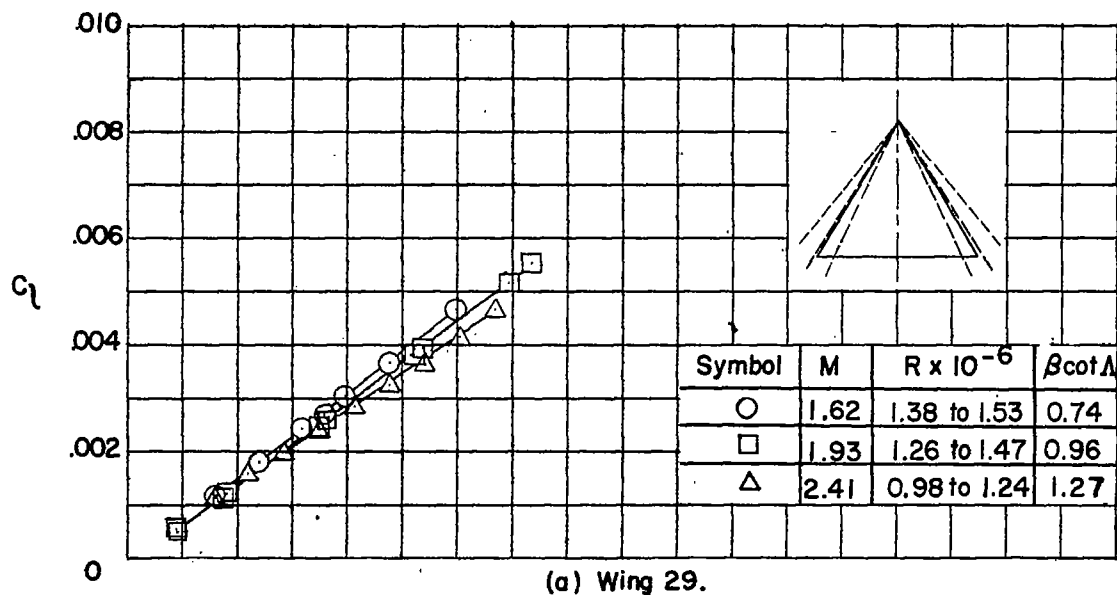


Figure 6.- Variation of rolling-moment coefficient with wing-tip helix angle for triangular wings. Flagged symbols indicate check points.

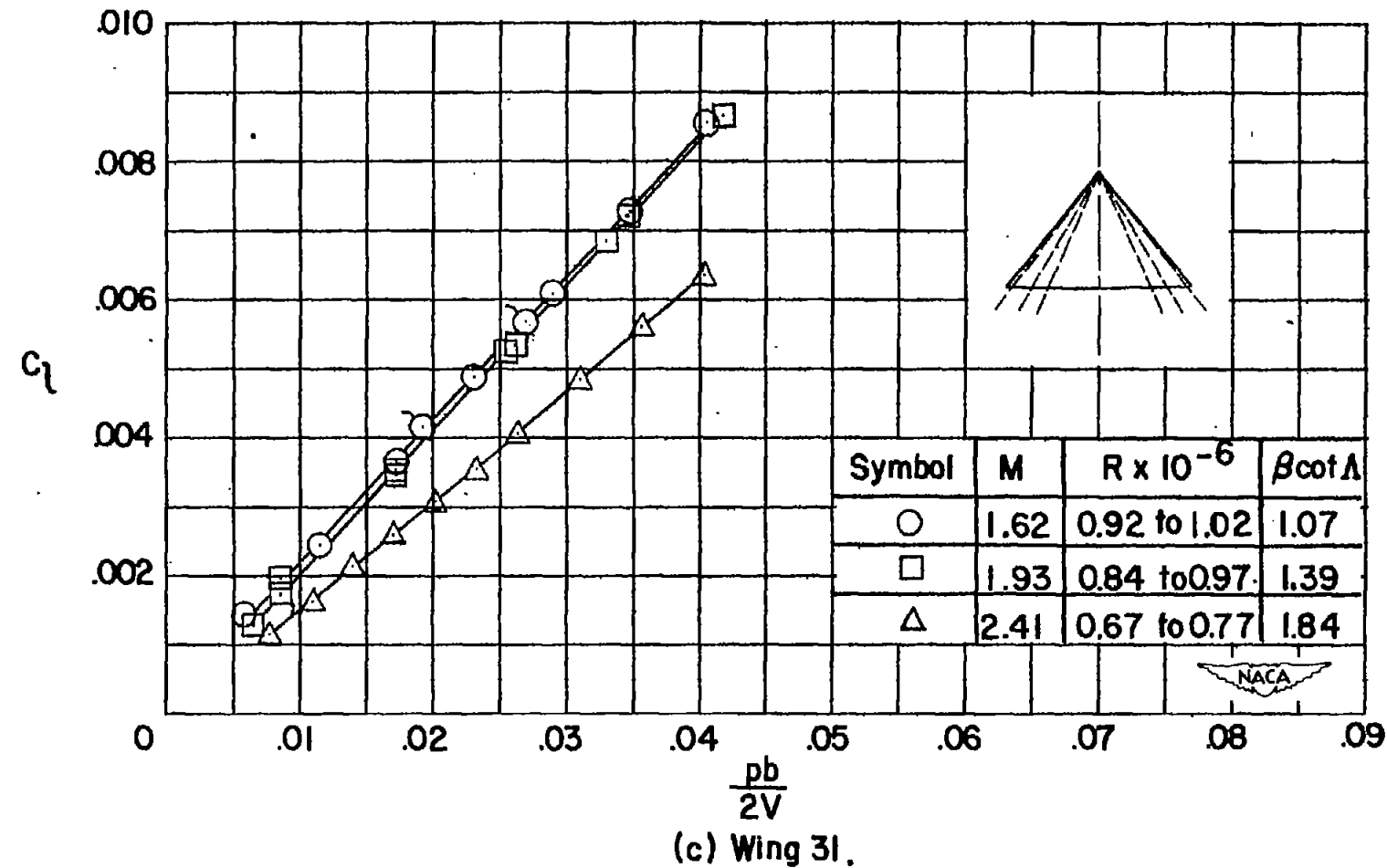


Figure 6.- Concluded.

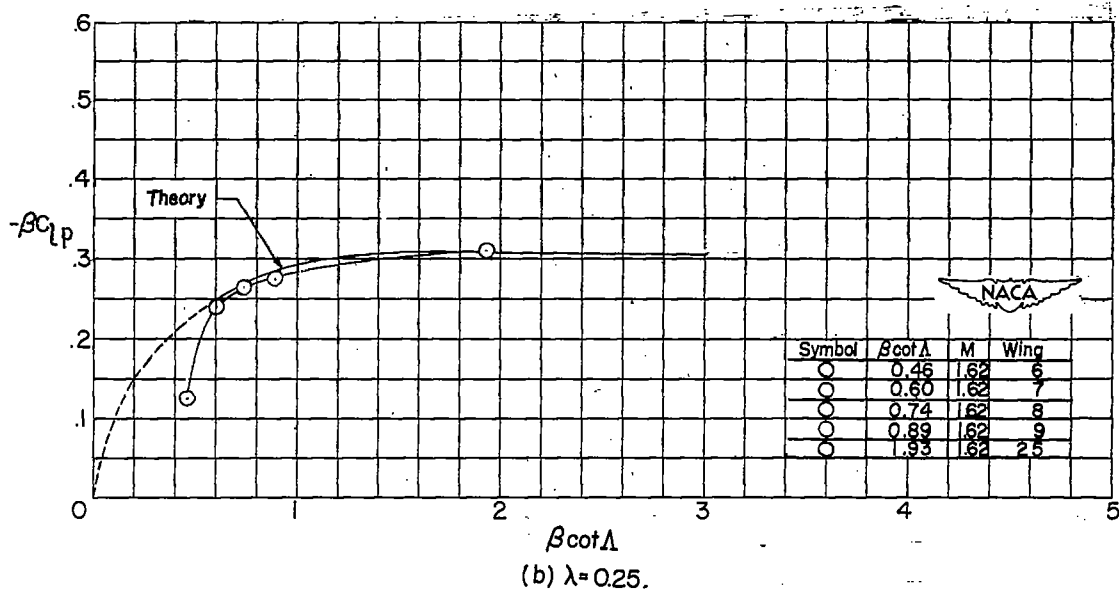
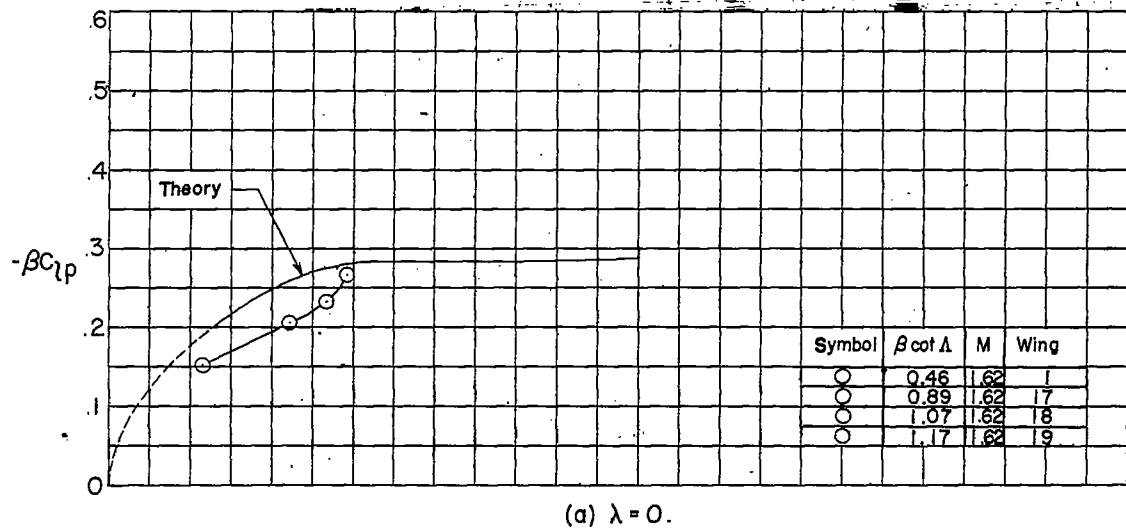


Figure 7.- Damping in roll of swept and tapered wings, $\beta A \approx 2.35$. Dashed portions of theoretical curves refer to wings with subsonic trailing edges and have limited significance.

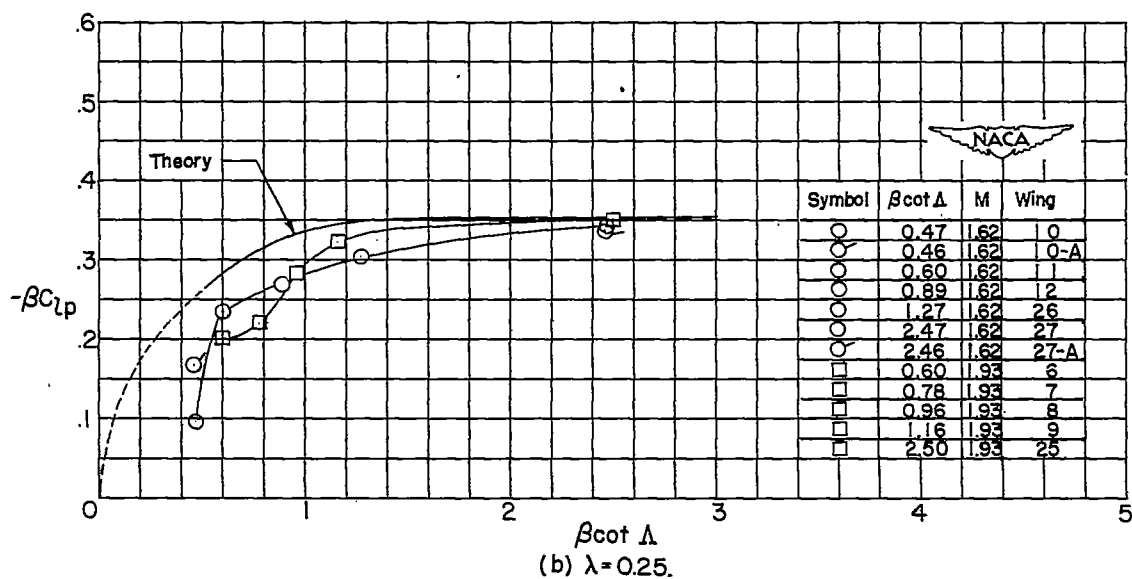
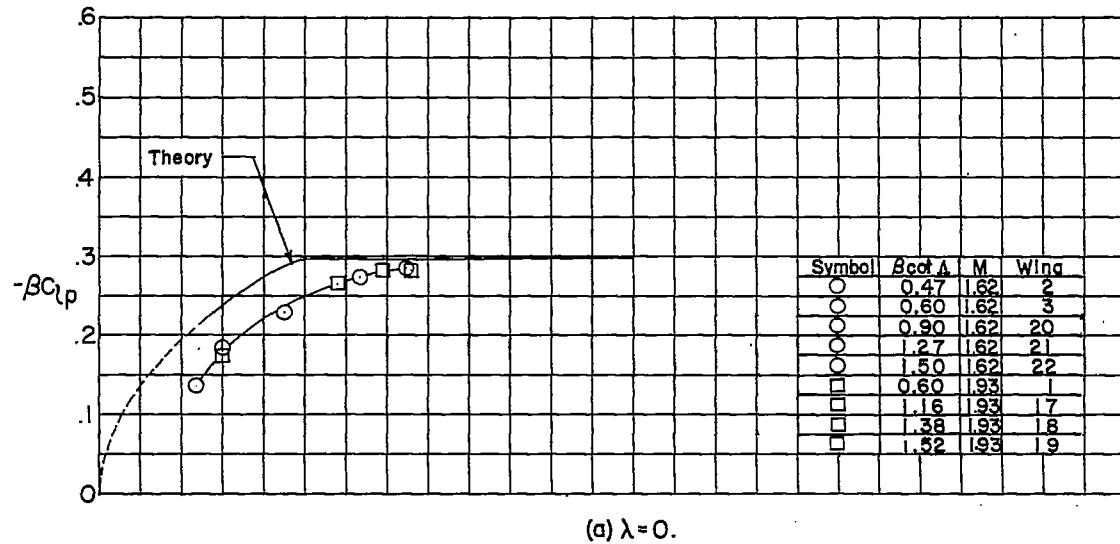


Figure 8.- Damping in roll of swept and tapered wings, $\beta A \approx 3.00$. Dashed portions of theoretical curves refer to wings with subsonic trailing edges and have limited significance.

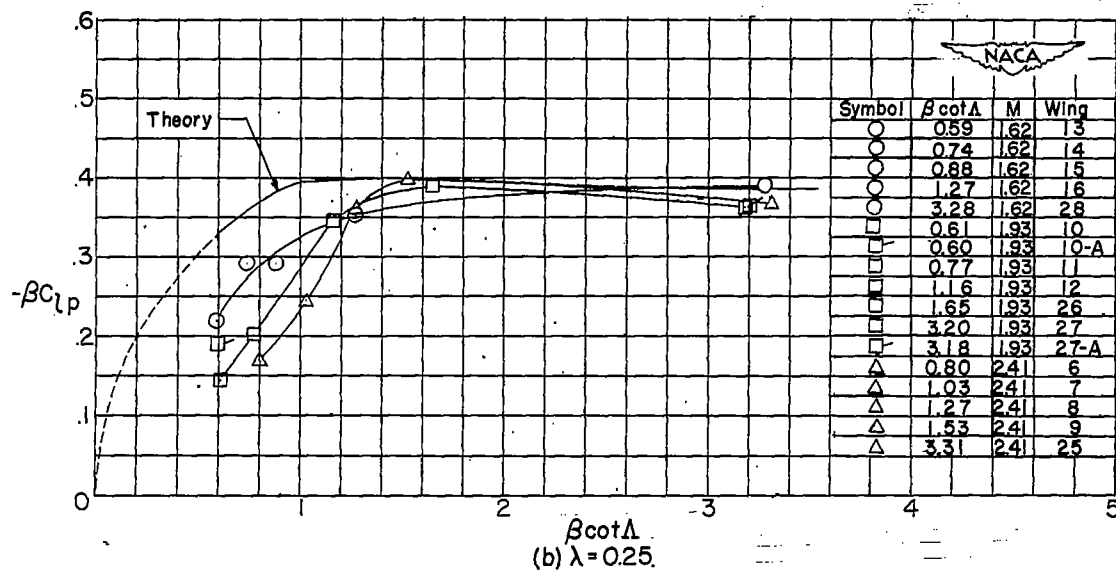
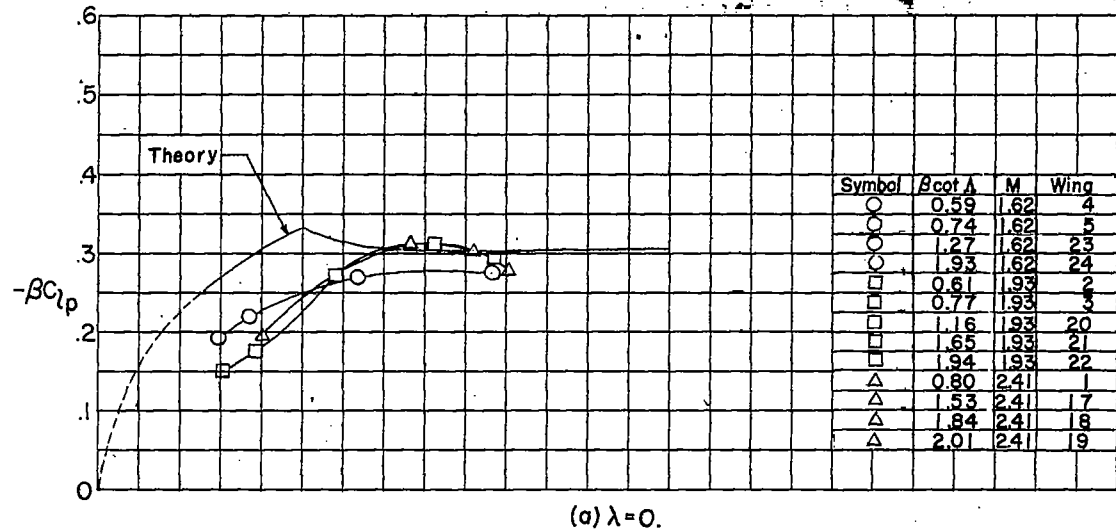


Figure 9.- Damping in roll of swept and tapered wings, $\beta \bar{A} \approx 4.00$. Dashed portions of theoretical curves refer to wings with subsonic trailing edges and have limited significance.

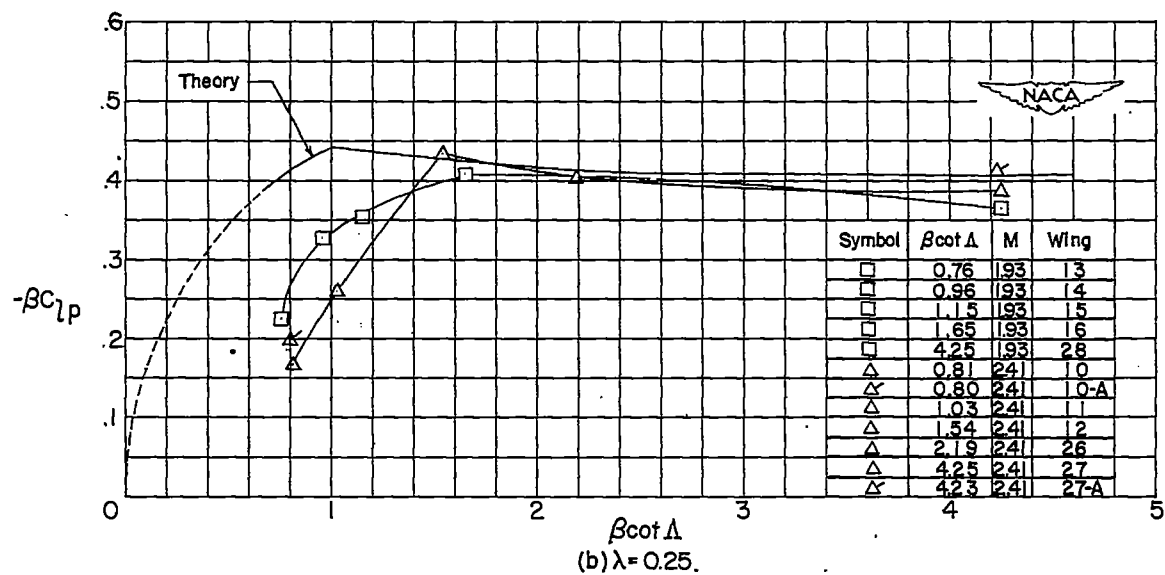
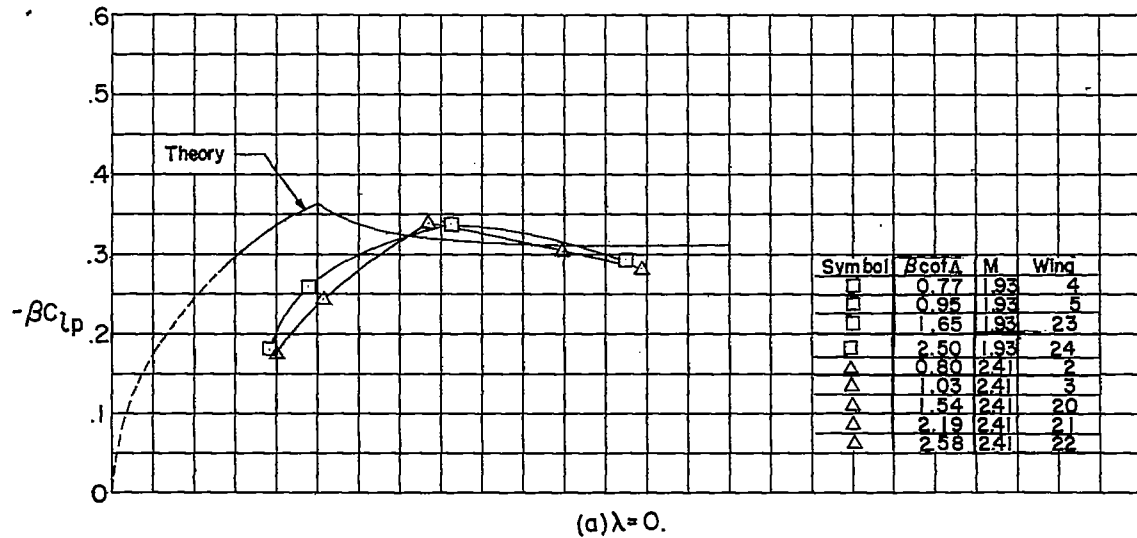


Figure 10.- Damping in roll of swept and tapered wings, $\beta A \approx 5.00$.
Dashed portions of theoretical curves refer to wings with subsonic trailing edges and have limited significance.

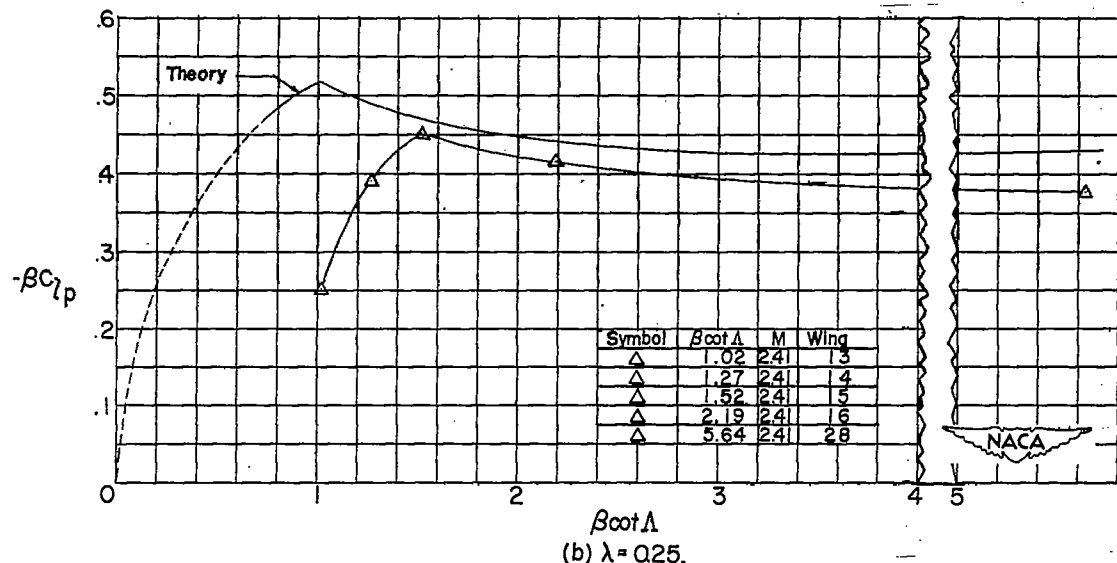
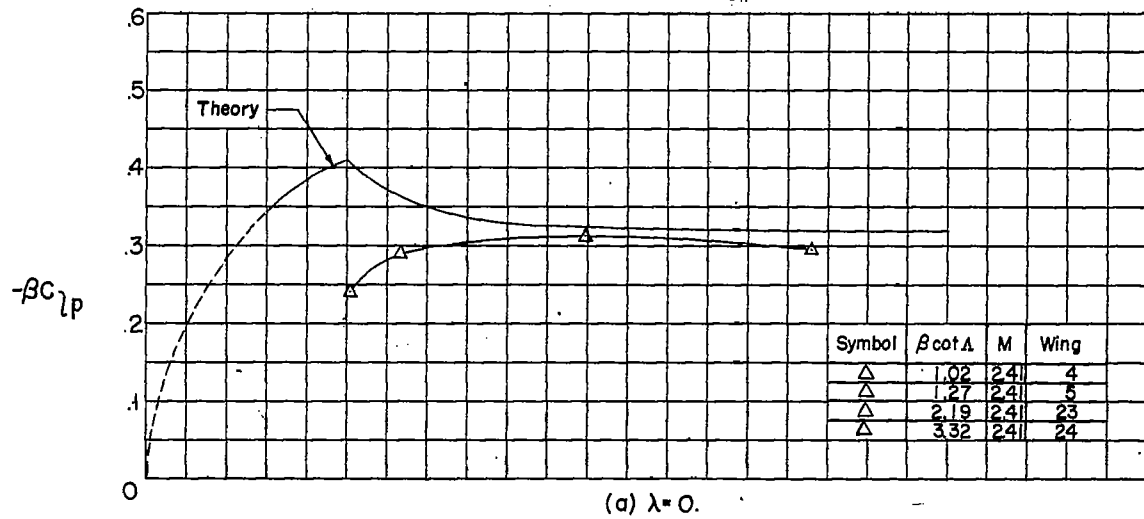


Figure 11.- Damping in roll of swept and tapered wings, $\beta A \approx 6.80$.
Dashed portions of theoretical curves refer to wings with subsonic trailing edges and have limited significance.

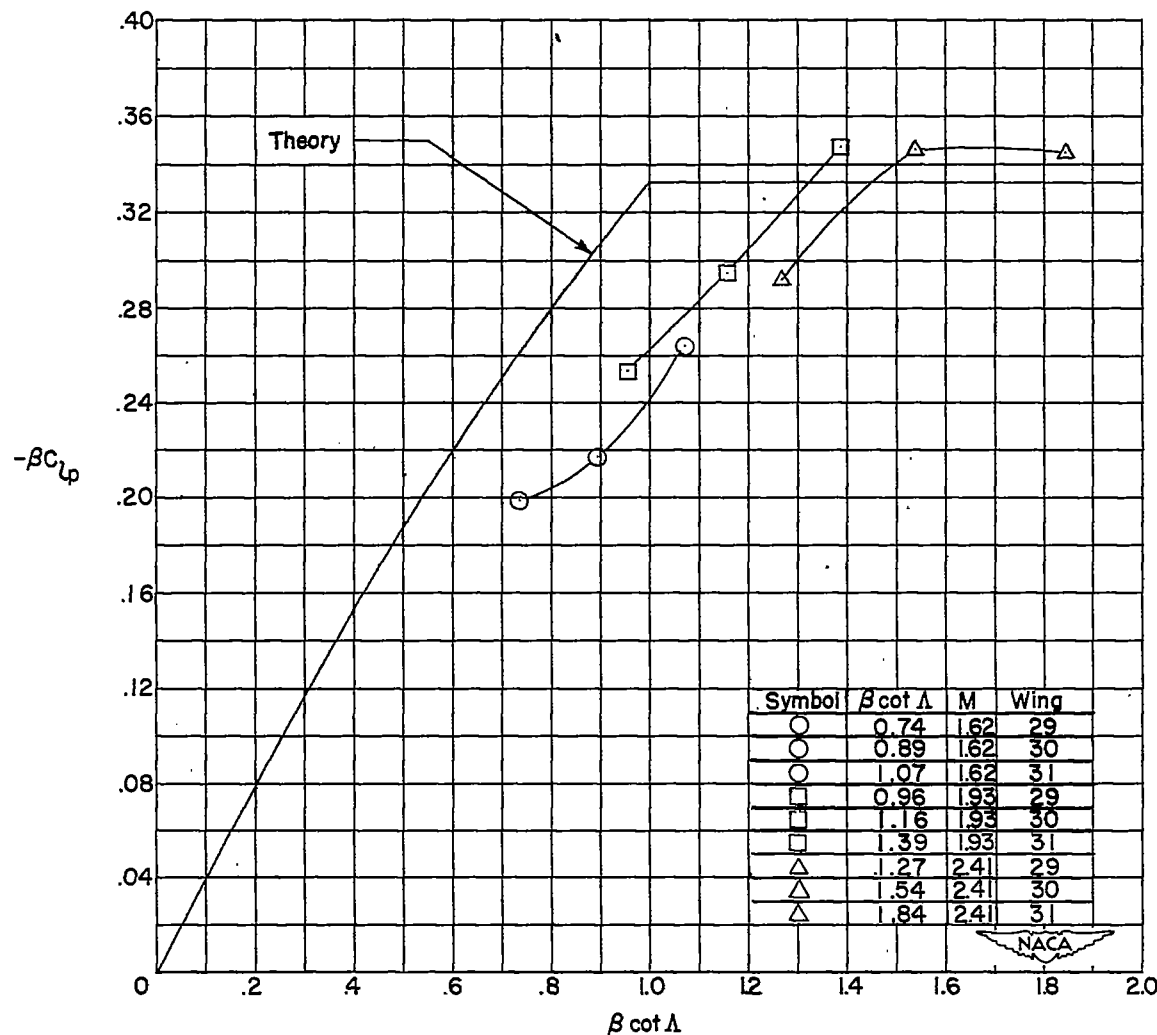


Figure 12.- Damping in roll of triangular wings.